博士学位論文

Development of π-Conjugated Carbon Molecules Grafted Silica Nano-particles Composite Materials

（π共役炭素分子をグラフトしたシリカナノコンポジット材料の開発に関する研究）

Yin Yang

Department of Applied Chemistry,
Graduate School of Engineering,
Kyushu Institute of Technology

2015

General Introduction

1.1 Background

1.1.1 Nano-materials

The essential differences in physic and chemical properties of nano-materials , compared to the bulk phase had been realized in lots of scientific and technological areas. The size-dependent tunable electronic, optical, magnetic and mechanical properties of nano-materials were basis to the current attractive and growing applications of nano-materials.[1] The most attentive nano-materials were arose from silica, noble metals, polymers, semiconductors, metal oxides, and carbon. Among such nano-materials, silica nano-particles, gold nano-particles, polymer nano-particles, semiconductor quantum dots, carbon nanotubes, nano-diamonds, fullerenes, and graphene are theme of basis research, device technology and biomedical technology. [2,3]The fluorescence, magnetic resonance, positron emission, photo-thermal and photo-acoustic effects, surface plasmon, and Raman and surface enhanced Raman scattering (SERS) were supplied by the above nano-materials enable us to resolve various problems in chemical, physical and biology science. [4]

Synthesis of colloidal nano-particles with unique optical and electronic properties, well-defined surface chemistry, well -controlled size and shape- distributions is the basis of all such applications. The large surface to volume ratios of nano-materials and their surface modifications using various chemical and bio-conjugate reactions have expanded applications (Fig.1).[5]

1.1.2 Silica nano-particles

Silica nano-particles can be classified into mesoporous and solid or non-porous. Because of chemical and physical stabilities, hydrophilic surface, well-defined surface
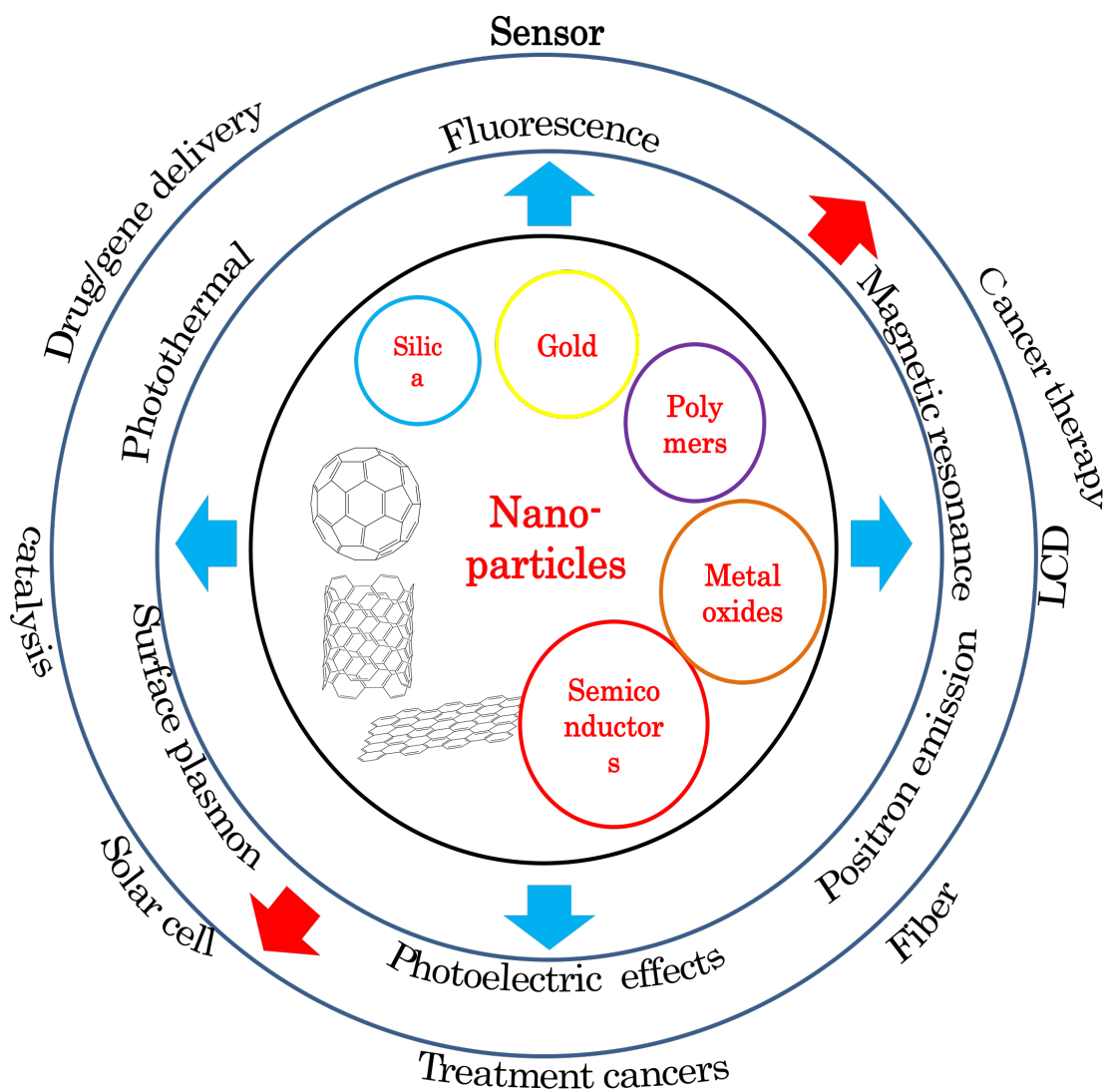
Fig. **1 Properties and application of nano-particles.**

chemistry, size-controlled synthesis rand large surface area, silica nano-particles have become common platforms for various chemical and catalytic reactions, and physical and biological applications. [6,7]

The Stöber process is a physical chemistry process for the generation of mono-disperse particles of silica.[2] The process was discovered in 1968 by Werner Stöber et al. Tetraethyl orthosilicate was added to an excess of water containing a low molar-mass alcohol such as ethanol and containing ammonia. Then, the resulting solution is stirred.[8] The resulting silica particles have diameters between 50 and 2000 nanometers depending on type of silicate ester used, type of alcohol used and volume ratios. The reactions taking place are hydrolysis of the silyl ether to a silanol followed by condensation reactions.[9] (Fig.2)

Mesoporous silica nano-particles are synthesized by the sol–gel process, which is *via* polymerization of silyl ethers stabilized in amphiphilic templates supplied by surfactants such as cetyltrimethyl ammonium bromide. The pore-size of mesoporou silica nano-particles thus synthesized can be controlled by changing the pH of the solution condition and composition of the solvents.[10,11]

1.1.3   Carbon materials

Carbon materials have observed ever-increasing research attention since over 20 years ago, when 0 D fullerene (C_{60}) and 1 D carbon nanotubes (CNTs) were discovered. In 2004, the successful isolation of monolayer 2D graphene (GR) caused a widely worldwide revolution target to apply the unique structural and electronic properties of GR to improve the performance of GR-based composite materials for aiming applications.[12] Therefore a great number of nano-structures have been composited with them and their derivatives.

5
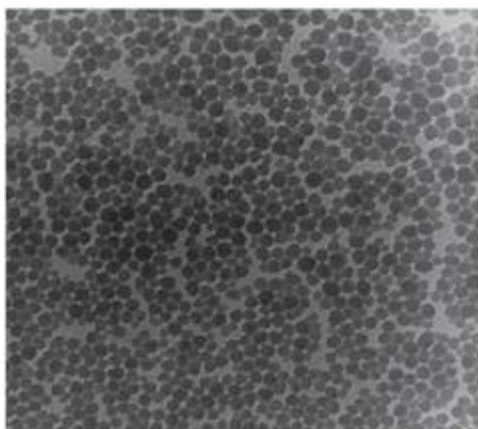
2a
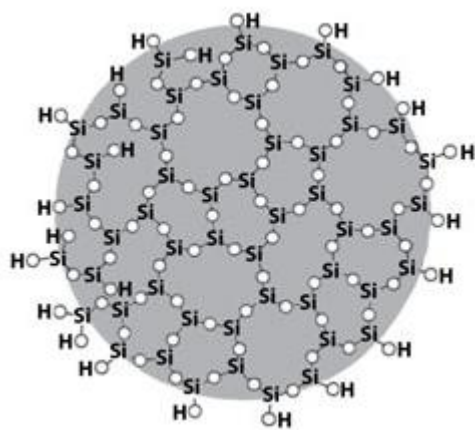
2b

Fig. 2 Transmission electron micrograph of silica nano-particles (2a) and Silica particles structure and surface (2b)

Carbon nanotubes (CNTs) were allotropes of carbon with a cylindrical nano-structure. Nanotubes had been constructed with length-to-diameter ratio of up to 132,000,000: 1, significantly larger than for any other material. These cylindrical carbon molecules had unusual properties, which were valuable for nanotechnology, electronics, optics and other fields of materials science and technology. In particular, owing to their extraordinary thermal conductivity and mechanical and electrical properties, carbon nanatubes found applications as additives to various structural materials. For instance, nanotubes formed a tiny portion of the materials in so baseball, golf clubs, car parts or damascus steel.[13]

Nanotubes were members of the fullerene structural family. Their name was derived from their long, hollow structure with the walls formed by one-atom-thick sheets of carbon, called graphene. There sheet were rolled at specific and discrete angles, and the combination of the rolling angle and radius decides the nanotube properties; for example, whether the individual nanotube shell was a metal or semiconductor. Nanotubes were categorized as single-walled nanotubes (SWNTs) and multi-walled nanotubes (MWNTs). Individual nanotubes naturally aligned themselves into ropes held together by van der Waals forces, more specifically, pi-stacking.[14]

A fullerene was a molecule of carbon in the form of a hollow sphere,ellipsoid, tube, and many other shapes. Spherical fullerenes were also called buckyballs, and they resemble the balls used in football (soccer). Cylindrical ones were called carbon nanotubes or buckytubes. Fullerenes are similar in structure to graphite, which was composed of stacked graphene sheets of linked hexagonal rings; but they might also contain pentagonal (or sometimes heptagonal) rings. [15]

The first fullerene molecule to be discovered, and the family's namesake, buckminsterfullerene (C_{60}), was prepared in 1985 by Richard Smalley,
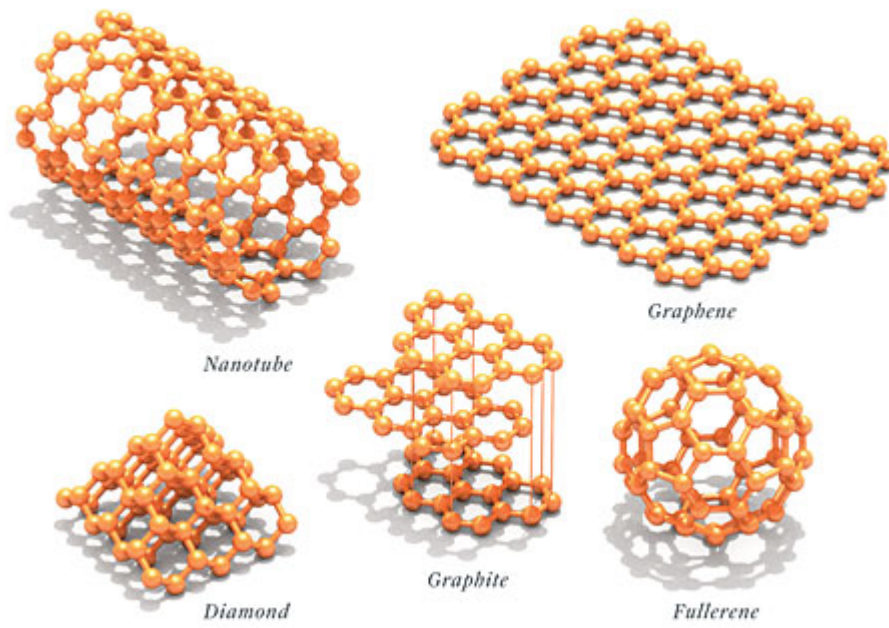
Fig. **3 The structure of carbon family.**

Robert Curl, James Heath, Sean O'Brien, and Harold Kroto at Rice University. The name was a homage to Buckminster Fuller, whose geodesic domes it resembles. The structure was also identified some five years earlier by Sumio Iijima, from an electron microscope image, where it formed the core of a "bucky onion." Fullerenes have since been found to occur in nature. More recently, fullerenes have been detected in outer space. According to astronomer Letizia Stanghellini, "It's possible that buckyballs from outer space provided seeds for life on Earth." [16,17]

Graphene is an allotrope of carbon, in the form of , a two-dimensional atomic-scale, hexagonal lattice in which one atom forms each vertex. It was the basic structural element of other allotropes, including graphite, charcoal, carbon nanotubes and fullerenes. [18]It could also be considered as an indefinitely large aromatic molecule, the limiting case of the family of flat polycyclic aromatic hydrocarbons.[19]

Graphene had many extraordinary properties. It was about 200 times stronger that steel by weight. Conducts heat and electricity with great efficiency and is nearly transparent. Researchers have identified the bipolar transistor effect, ballistic transport of charges and large quantum oscillations in the material.[20]

1.1.4 Carbon materials composite

In the last few decades, great efforts have been made to synthesize inorganic nanostructures with controlled shape, size, crystallinity and functionality. These materials were widely employed in applications like optics, electronics, storage, solar energy harvesting and electrochemical energy conversion and so on. In order to further enhance their properties, a great number of inorganic nanostructures have been composited with carbon family and its derivatives, which include metals like Au, [21] Ag,[22] Pd,[23] Pt,[24] Ni,[25] Cu,[24] Ru[26] and Rh[26] oxides like TiO_2,[27] ZnO,[28] SnO_2,[29] MnO_2,
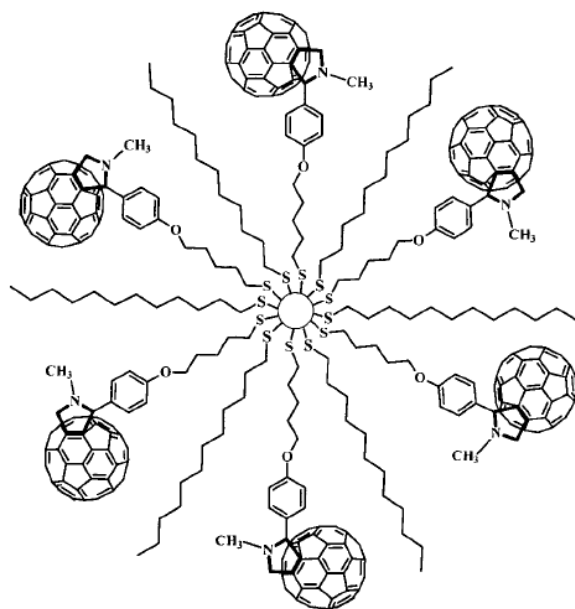
4a
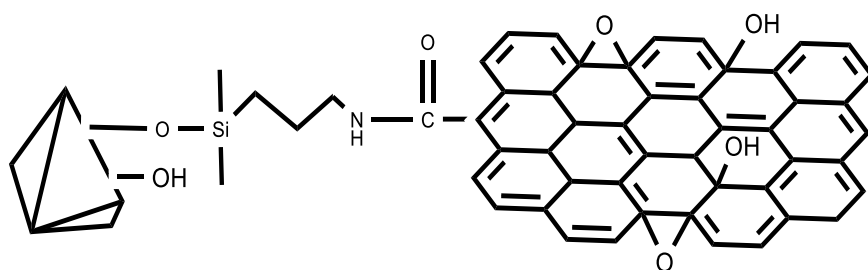
4b

Fig. 4 Functionalize a gold nanoparticle with a thiol derivative of fullerene (4a) and

G and GO supported on silica (4b).

$^{30}Co_3O_4,^{31}Fe_3O_4,^{32}$ NiO,^{33} Cu$_2$O, ^{34}RuO$_2$^{35} and SiO$_2$^{36}chalcogenides like CdS^{37} and CdSe.^{38}

At present, almost of these composite nano-structure are synthesized via blend be conjugated with surface groups, or post-synthesis surface groups which are exhibited many reports, and they shows broad application prospect. As shows (Fig.4):

S. Barazzouk, S. Hotchandani reported a self-assembled photoactive antenna system containing a gold nano-particle as the central nanocore and appended fullerene moieties as the photoreceptive hydrophobic shell was designed by functionalizing a gold nano-particle with a thiol derivative of fullerene. The quenching of fluorescence emission as well as decreased yields of triplet excited state suggested the participation of excited singlet in the energy transfer to the gold nanocore. Application of electro-phoretically deposited Au−S−C$_{60}$ nanoassemblies on optically transparent electrodes in the photo-electrochemical conversion of light energy has been illustrated. ^{39}(Fig. 4a)

Q. Liu, J. Shi reported that they have demonstrated that G and GO supported on silica provide a versatile and high-performance platform for SPE towards various analytes ranging from small molecules of pollutants to biomolecules such as proteins and peptides. Notably, G bound silica is capable of extracting sticky proteins with large molecular weight and phosphorylated peptides, making them particularly suitable for handling biological samples for MALDI-TOF MS analysis. Our results further reveal the remarkable potential of G-based materials for sorption applications. ^{40}(Fig. 4b)

1.2 This paper

We have successfully achieved colloidal crystallization of polymer-grafted silica in

11

organic solvents and then immobilization in polymer matrix. [41-44]Polymer grafting techniques provide a very versatile tool to tailor the surface of nanoparticles and thus the interfaces between nano-particles and the matrix polymers.[45-49] In order to develop this area further, we utilize polymer to modify the silica surface, and then tether the silica with carbon family, target conveniently adjust the ratio of carbon molecules and nano-particles and fine-turning the proprieties.

We graft the fullerene and graphene with the polymer modified silica, respectively. After preparation of C_{60}-tethered polymer-grafted silica (C_{60}/polymer/ SiO_2), the colloidal crystallization of the composite particles in organic solvent was investigated. Moreover, the silica -tethered polymer-grafted graphene (SiO_2/polymer/graphene) was synthesized, and well dispersion was obtained.

This thesis consisting of four chapters is a summary of the author's work. An outline of each chapter is described below.

In **chapter 1**, in order to enable us to combine silica nano-particles and carbon molecules, we design and synthesize a difunctional polymer. 3-mercapto- propyl triethoxy silanes are extensively employed in condensation reactions, which thiol groups on the surface of silica nanoparticles. 4-azidobenzoly chloride both with acyl chloride and azido group are employed in react with polymer and π-conjugated molecule, respectively. Due to chemical and physical stabilities, PMMA are extensively employed in various areas. HEMA with almost same advantage with MMA, on the other hand, could react with both thiol groups. For the sake of adjust the ratio and control the performance, we put two functional groups on the terminal and the side chain, respectively. The silica nano-particles own stabilities chemical and physical properties and the 3-mercaptopropyl triethoxy silane also could be a transfer

reagent. So placed on the terminal is the best choice. On the other hand, the acyl chloride groups with little instability, placed on the side, in favor of the reaction with π-conjugated molecule.

In **Chapter 2**, we show that synthesis of fullerene (C_{60})-tethered polymergrafted silica and colloidal crystallization of the particles was investigated. The particles were prepared by the reaction of C_{60} with 4-azidobenzoyl groups introduced in poly(methyl methacrylate-*co*-2-hydroxyethyl methacrylate). The reaction afforded bindings of C_{60} in the range from 0.44×10^4 to 1.71×10^4 molecules/particle. The C_{60} amounts did not monotonously increase with 4-azidobenzoyl group on the particles, but decreased with mole fraction of methyl methacrylate in the copolymer.

In **chapter 3,** we prepare C_{60}-tethering polymer-grafted silica and colloidal crystallization in organic solvent were investigated. Critical volume fraction and reflection spectra were evaluated. Inter-sphere distances in the colloidal crystals mostly agreed with calculated values on assumption of fcc-closed packing. Therefore, it was suggested that the crystallization occurred due to electrostatic repulsion between the particles as well as those of colloidal silica particles in aqueous solution.

In **chapter 4**, we have done a basic study of a graphene – polymer /SiO_2 system, polymer-grafted silica spheres-tethered graphene nano-sheet composite material, which were prepared by the reaction of graphene with 4-azidobenzoyl groups introduced in poly (methylmethacrylate-*co*-2-hydroxyethyl methacrylate), synthesized *via* a radical copolymerization, followed by esterification of 2-hydroxyethyl metharylate moieties with 4-azidobenzoyl chloride and grafted with colloidal silica. We found that the graphene/poly(MMA-*co*-AEMA)/SiO_2 was well dispersion in many solvents.

Reference

1　V. Biju *Chem. Soc. Rev.,* **2014**, 43, 737-962

2　B. G. Trewyn, I. I. Slowing, S. Giri, H.-T. Chen and V. S.-Y. Lin, *Acc. Chem. Res.*, **2007**, 40, 846–853

3　S.-H. Wu, C.-Y. Mou and H.-P. Lin, *Chem. Soc. Rev.*, **2013**, 42, 3862–3875.

4　A. Vinu, K. Z. Hossain and K. Ariga, *J. Nanosci. Nanotechnol.*, **2005**, 5, 347–371.

5　G. T. Hermanson, Bioconjgate Techniques, *Academic Press*, **1996**.

6　P. Yang, S. Gaib and J. Lin,Chem. *Soc. Rev.*, **2012**, 41, 3679–3698.

7　Z. Li, J. C. Barnes, A. Bosoy, J. F. Stoddar and J. I. Zink, Chem. *Soc. Rev.*, **2012,** 41, 2590–2605.

8　T. J. Yoon, K. N. Yu, E. Kim, J. S. Kim, B. G. Kim, S. H. Yun, B. H. Sohn, M. H. Cho, J. K. Lee and S. B. Park, *Small*, **2006,** 2, 209–2015

9　T. Padmavathy, P. Keith and S. Swadeshmukul, *Nanomedicine*,**2008,** 3, 579–592

10　P. Couleaud, V. Morosini, C. Frochot, S. Richeter, L. Raehm and J. O. Durand, *Nanoscale*, **2010**, 2, 1083–1095.

11　E. S. Shibu, M. Hamada, N. Murase and V. Biju, *J. Photochem. Photobiol., C*, **2013**, 15, 52–73.

12　Novoselov, K. S. Geim, A. K., Morozov, S. V.; Jiang, D.; Zhang,Y.; Dubonos, S. V.; Grigorieva, I. V. Firsov, *A. A. Science* **2004**, 306, 666−669.

13　Wang, X.; Li, Qunqing; X, Jing; J, Zhong, W. Jinyong, L. Yan; J. Kaili; F. Shoushan. *Nano Letters* **2009**, 9, 3137–3141.

14　S. Gullapalli, M.S, Wong., *Chemical Engineering Progress* **2011**,107, 5, 28–32.

15　S. Iijima. *Journal of Crystal Growth* **1980**,50 ,3, 675.

16　P.R. Buseck, S.J. Tsipursky, R. Hettich. *Science* **1992**,257, 5067, 215–7.

17　J. Cami, J. Bernard-Salas, E. Peeters, S. E. Malek. *Science* **329** , 5996, 1180–2.

18 S. V. Morozov, K. S. Novoselov, M. I. Katsnelson, F. Schedin, D. C. Elias, J. A. Jaszczak, A. K. Geim. *Phys. Rev. Lett*. **2008,** 100016602.

19 M. D. Stoller, S. Park, Y. Zhu, J. An, R. S. Ruoff. *Nano Lett* ,**2008**, 8, 3498−3502.

20 X. Li, Y. Zhu, W. Cai, M. Borysiak, B. Han, D. Chen, R.D. Piner, L. Colombo, R. S. Ruoff. *Nano Lett.* **2009**, 9, 4359−4363.

21 X. Zhou, X. Huang, X. Qi, S. Wu, C. Xue, F. Y. C. Boey, Q. Yan P. Chen and H. Zhang, *J. Phys. Chem. C*, **2009**, 113 10842–10846.

22 J. Huang, L. Zhang, B. Chen, N. Ji, F. Chen, Y. Zhang and Z. Zhang, *Nanoscale,* **2010,** 2, 2733–2738.

23 H. M. A. Hassan, V. Abdelsayed, A. Khder, K. M. AbouZeid, *J. Mater. Chem.,* **2009**, 19, 3832–3837.

24 J. B. Liu, S. H. Fu, B. Yuan, Y. L. Li and Z. X. Deng, *J. Am. Chem. Soc.*, **2010**, 132, 7279–7281

25 H. Wang, J. T. Robinson, G. Diankov and H. Dai, *J. Am. Chem. Soc.*, **2010**, 132, 3270–3271

26 D. Marquardt, C. Vollmer, R. Thomann, P. Steurer, R. Mu lhaupt, E. Redel and C. Janiak, *Carbon*, **2011**, 49,1326–1332..

27 J. Liu, H. Bai, Y. Wang, Z. Liu, X. Zhang and D. D. Sun, *Adv. Funct. Mater.*, **2010**, 20, 4175–4181.

28 Z. Yin, S. Wu, X. Zhou, X. Huang, Q. Zhang, F. Boey and H. Zhang, *Small*, **2010**, 6, 307–312.

29 D. Wang, R. Kou, D. Choi, Z. Yang, Z. Nie, J. Li, L. V. Saraf. *ACS Nano*, **2010**, 4, 1587–1595.

30 S. Chen, J. Zhu, X. Wu, Q. Han and X. Wang, *ACS Nano*, **2010**,4, 2822–2830

31 Z.-S. Wu, W. Ren, L. Wen, L. Gao, J. Zhao, Z. Chen, G. Zhou, F. Li and H.-M.

Cheng, *ACS Nano*, **2010**, 4, 3187–3194.

32　J. F. Shen, Y. Z. Hu, M. Shi, N. Li, H. W. Ma and M. X. Ye, *J. Phys. Chem. C,* **2010**, 114, 1498–1503.

33　J. Y. Son, Y.-H. Shin, H. Kim and H. M. Jang, *ACS Nano*, **2010**,4, 2655–2658

34　S. Wu, Z. Yin, Q. He, X. Huang, X. Zhou and H. Zhang, *J. Phys. Chem. C*, **2010**, 114, 11816–11821

35　F. Kim, J. Luo, R. Cruz-Silva, L. J. Cote, K. Sohn and J. Huang, *Adv. Funct. Mater.*, **2010**, 20, 2867–2873.

36　S. Watcharotone, D. A. Dikin, S. Stankovich, R. Piner, I. Jung, C. P. Liu, S. T. Nguyen and R. S. Ruoff, *Nano Lett.*, **2007**, 7, 1888–1892

37　M. Feng, R. Q. Sun, H. B. Zhan and Y. Chen, *Nanotechnology*, **2010**, 21, 075601

38　Y. T. Kim, J. H. Han, B. H. Hong and Y. U. Kwon, *Adv. Mater.*,**2010**, 22, 515–518

39　H. Imahori,　K. Mitamura, *J. Phys. Chem. B,* **2006,** *110,* 11399-11405

40　Q. Liu, j. Shi, J. Sun, T. Wang. *Angew. Chem*. **2011**, 123, 6035-6039

41　M. Chiyoda, A. Yoneda, H. Nishida. *Colloid Polym Sci*,**1999,**277, 479–482

42　K. Yoshinaga, M.Chiyoda, T. Okubo. *Colloids Surf,***2002** , 204,285–293

43　K. Yoshinaga, K. Fujiwara,Y. Tanaka, M. Nakanishi, M. Takesue. *Chem Lett.* **2003**,32,1082–1083

44　K.Yoshinaga, M. Shigeta, S. Komune, E. Mouri, A. Nakai. *Colloids Surf B*,**2007**,54, 108–113

45　Yoshinaga K, Mouri E, Ogawa J, Nakai A, Ishii M, Nakamura H; *Colloid Polym Sci* ,**2004**,283,340–343

46　Yoshinaga K, Fujiwara K, Mouri E, Ishii M, Nakamura H *Langmuir* ,**2005,**21, 4471–4477

47 Yoshinaga K, Satoh S,Mouri E, Nakai A; *Colloid Polym Sci* ,**2006**,285,694–698

48 Ma Z,WatanabeM,Mouri E, Nakai A, Yoshinaga K, *Colloid Polym Sci*,**2011**, 289,85–91

49 Yoshinaga K, Chiyoda M, Yoneda A, Nishida H, Komatsu M ;*Colloid Polym Sci,***1999,** 277,479-482

Chapter 1

Synthesis of Trimethoxysilyl-capped and
4-Azidobenzoyl Groups Modified Difunctional Polymer

1.1 Introduction

Polymer grafting techniques provided a very capable tool to modify the surface of nano-particles and thus the interfaces between nano-particles and the matrix polymers. These techniques provided control over the type of polymer to be grafted onto the particle surface, surface densities, and chain lengths at the nanometer scale.[1] The techniques of covalently grafting polymer chains onto particles could be classified into "grafting from" and "grafting to". The grafting from technique uses initiators that have been initially anchored to the particle surface, followed by the polymerization from the surface.[2,3] On the other hand, the grafting to technique involved reacting the polymer, bearing an suitable functional group, with the particles to chemically added the polymer chains.[4,5] Due to the steric hindrance increased with the already grafted chains, it becomes increasingly difficult for the incoming polymer chains to diffuse to the surface against the concentration gradient of the existing grafted polymers, which results in low graft densities.

In **chapter 1**, in order to enable us to combine silica nano-particles and carbon molecules, we design and synthesize a difunctional polymer. Various trialkoxysilanes are extensively employed in condensed with the surface silanol group.[6] 3-mercaptopropyl triethoxy silanes are extensively employed in condensation

reactions, which thiol groups on the surface of silica nanoparticles.[7] The direct condensation of silane-functionalized molecules such as dye, DNA, siRNA, polymer, gold, QD, etc.4-azidobenzoly chloride both with acyl chloride and azido group are employed in react with polymer and π-conjugated molecule, respectively.[8,9]Due to chemical and physical stabilities, PMMA are extensively employed in various areas. HEMA with almost same advantage with MMA, on the other hand, could react with both thiol groups. [10,11]

For the sake of adjust the ratio and control the performance, we put two functional groups on the terminal and the side chain, respectively. The silica nano-particles own stabilities chemical and physical properties and the 3-mercaptopropyl triethoxysilane also could be a transfer reagent. [12,13] So placed on the terminal is the best choice. On the other hand, the acyl chloride groups with little instability, placed on the side, in favor of the reaction with π-conjugated molecule.

1.2 Experimental Section

1.2.1 Materials

Methyl methacrylate (MMA) and 2-hydroxyethyl methacrylate (HEMA), (3-mercaptopropyl) trimethoxysilane, 2,2′-azobis(isobutyronitrile) (AIBN), tetrahydrofuran (THF), Chloroform, were obtained from Wako Chemicals Co. Ltd., Osaka, Japan

1.2.2 Synthesis of trimethoxysilyl-capped and 4-azidobenzoyl groups modified difunctional polymer

A typical run was as follows. A mixture of 12.0 mL　(112 mmol) MMA, 0.68 mL (5.6 mmol) HEMA, 10 mg　(0.07 mmol) (3-mercaptopropyl)trimethoxysilane, 16 mg

(0.17 mmol) AIBN, and 20 mL dry THF was put into a 50-mL flask and stirred at 70 °C for 10 h in N_2 atmosphere. After evaporation of THF from the mixture and precipitation with diethyl ether, drying under reduced pressure gave 7.2 g copolymer Poly(MMA-*co*-AEMA), of Mn 24,000 and MMA/HEMA mole ratio 14.7:1.0. The mole ratio was determined by the area ratio of resonance peak at 3.63 ppm assigned to methyl protons of MMA moiety to peaks at 3.87 and 4.15 ppm assigned to methylene protons of HEMA moiety on 1H NMR spectrum. 1H NMR ($CDCl_3$): 0.87, 1.05, 1.23 (m, CH_3), 1.76–2.15 (broad, CH_2, CH), 3.63 (s, OCH_3), 3.87 (broad, $COOCH_2$), and 4.15 ppm (broad, CH_2OH).

1.2.3 Synthesis of trimethoxysilyl-capped poly(methyl methacrylate--*co*-2-(4-azidobenzoyloxy)ethyl metharylate)

Into a 50-mL flask, 2.0 mL *N,N,N*-triethylamine, 3.0 g poly(MMA-*co*-HEMA), and 30 mL dry chloroform were put, and the mixture was cooled on an ice bath. Chloroform solution 2.0 mL containing 3 g (17 mml) 4-azidobenzoyl chloride was added dropwise to the solution, followed by stirring for 6 h at room temperature. Filtration, evaporation of solvent, and precipitation with diethyl ether gave 2.45 g 2. 1H NMR ($CDCl_3$): 0.87, 1.05, 1.23 (m, CH_3), 1.76–2.15 (broad, CH_2, CH), 3.63 (s, OCH_3), 3.87 (broad, $COOCH_2$), 4.15 (broad, CH_2OH), 4.32 (broad, $COOCH_2CH_2OC=OC_6H_4N_3$), 4.55 (broad, $CH_2OC=OC_6H_4N_3$), 7.18 (broad, o−CH_2 ($C=OC_6H_4N_3$)), and 8.09 ppm (board, m–CH_2 ($C=OC_6H_4N_3$)).

1.2.4 Polymer characterization

Number average of molecular weight (Mn) of the synthesized polymers were determined by a gel permeation chromatography (GPC) on the columns, TSK gel
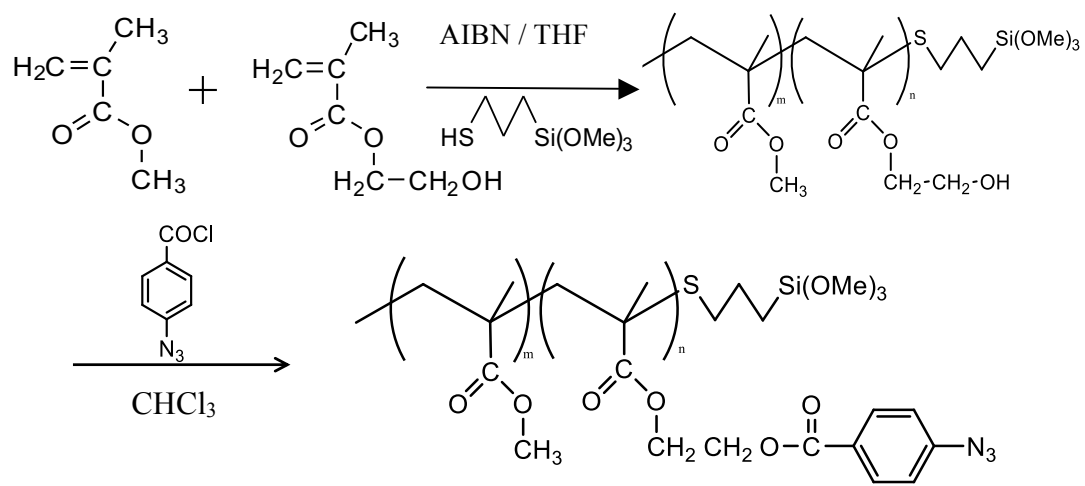
Scheme 1　The synthetic route of poly(MMA-*co*-AEMA).

G4000H6, and G5000H6, Tosoh Co. Ltd., Yamaguchi, Japan, a 35 °C using THF as an

eluent at the flow rate of 0.8 mL/ min calibrated with a polystyrene standard. Molecular

weights were calculated with the aid of polystyrene standards.^{1}H NMR spectra for

solution samples were recorded on a Bruker AVANCE 400 (400 MHz), 5-10%

(solutions) in CDCl$_3$ with Si(CH$_3$)$_4$ as an internal standard were recorded at room

temperature.

1.3 Result and discussion

In Scheme 1, The synthetic route of poly(MMA-*co*-AEMA) was shown.

Trimethoxysilyl-terminated poly(MMA-*co*-HEMA) was synthesized by a radical

copolymerization of MMA and HEMA in the presence of (3-mercaptopropyl)

trimethoxysilane of a chain transfer reagent using AIBN as an radical initiator at 70°C

for 10 h in N$_2$ atmosphere.[14,15]

For the ^{1}HNMR spectra (Fig.5), the introduction of HEMA group was confirmed by

the appearance of peaks at 3.87 and 4.15*ppm*, the introduction of MMA group was

confirmed by the appearance of peaks at 3.65*ppm*. For the appearance of multiple peaks

from 0.8 ~ 2.0*ppm*, it was suggested that the poly(MMA-*co*-HEMA)was synthesized

successfully. The ratios of MMA to HEMA were determined from the area ratio of

peaks at 3.87 and 4.15ppm to 3.65ppm. (Table 1)

The number-average molecular weights of polymers were obtained from gel

permeation chromatography (GPC) measurements. A typical GPC traces of the

poly(MMA-*co*-HEMA) as show as in Fig. 6. For the appearance of peak at 8 min

to10min, it was suggested that the Mn value of poly(MMA-*co*-HEMA) was 24,000

and Mw/Mn was 1.58.The molecular weight distribution is narrow and unimodal,

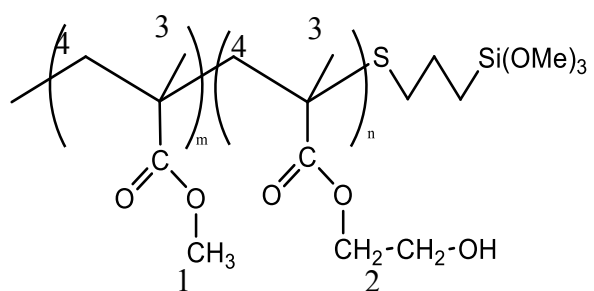indicating that the polymerization was performed in a controlled manner.[16,17]

Table 1 ^{1}H NMR chemical shifts of Poly(MMA-*co*-HEMA).

δ (ppm)	Assignment
3.6	**1**
3.8 , 4.1	**2**
0.8 ~ 1.0	**3**
1.5 ~ 2.0	**4**

Poly(MMA-*co*-HEMA)

MMA : HEMA = 1.9 : 1.0
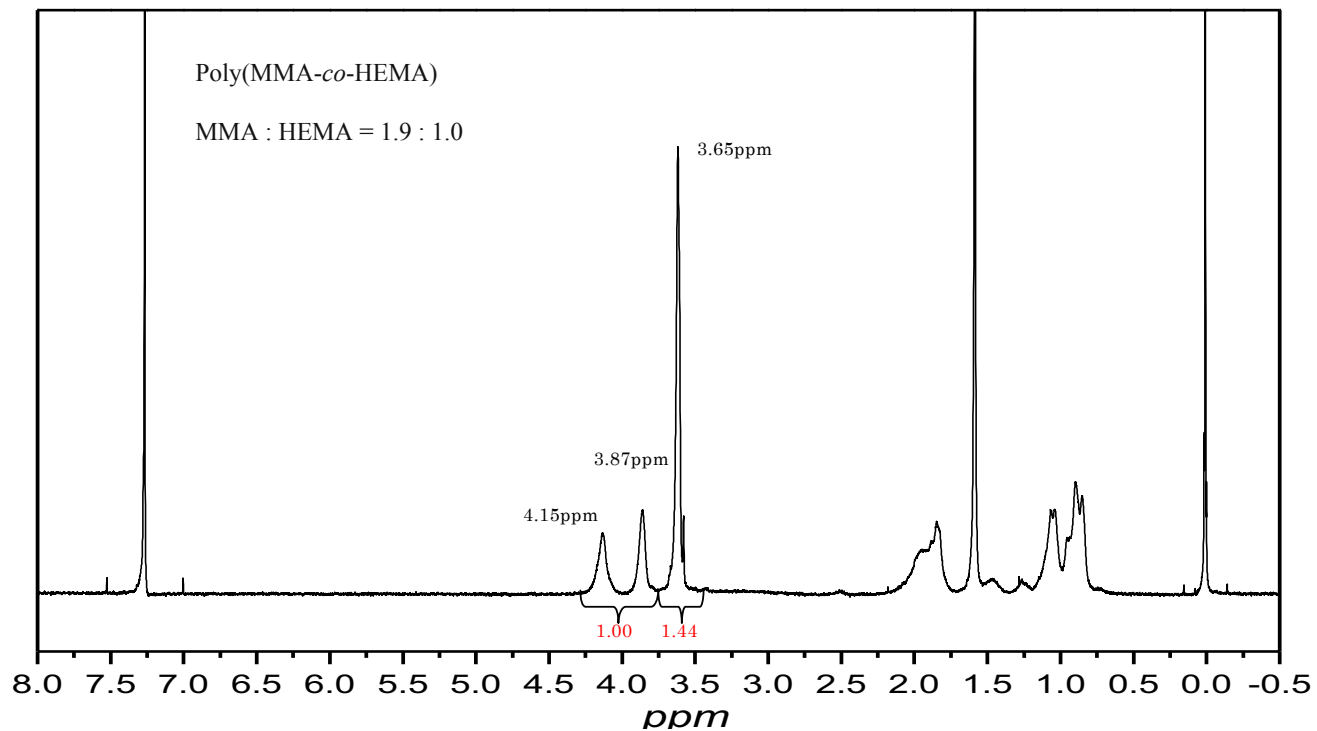
3.65ppm

3.87ppm

4.15ppm

1.00   1.44

Figure 5 Typical 1H NMR spectra of poly(MMA-co-HEMA) with mole ratio of MMA/HEMA=1.9:1.0
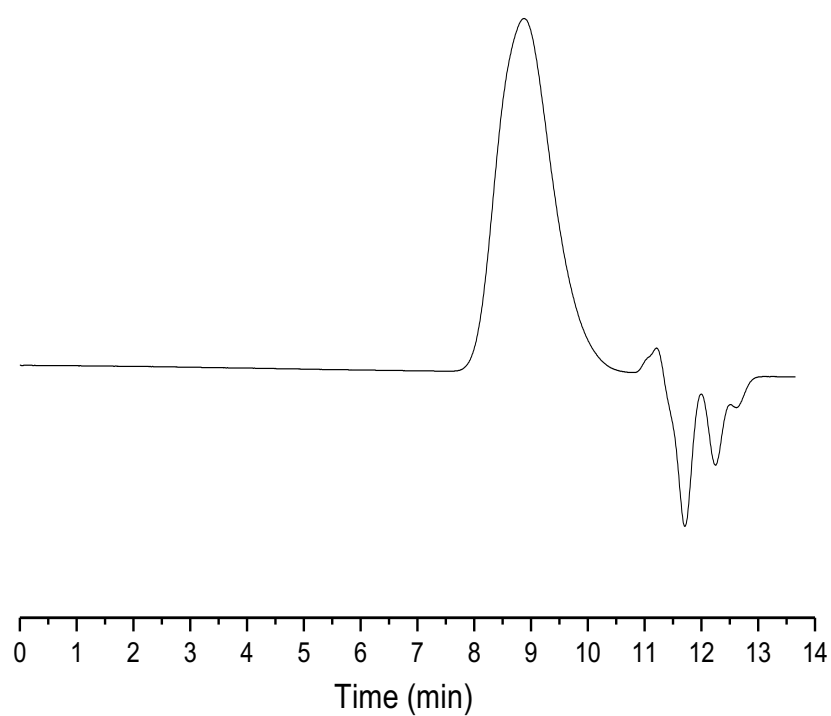
Fig. 6 Gel permeation chromatograms of Poly(MMA-*co*-HEMA)

For the table 2, the polymer of Mn=11,000~24,000 with mole ratios of

MMA/HEMA in the range from 1.9:1.0 to 14.7:1.0 were obtained by changing feed

ratio of the monomers (Fig.7-10). In order to reduce the number-average molecular

weight influence on performance evaluate later, need to hold the Mn in a similar

values. Due to changing feed ratio of the monomers, the polymer of Mn = 11,000 ~

16,000 were obtained as shows as No.1 to No.4. For research the influence of high

number-average molecular weight, a polymer of Mn = 24,000 was also obtained as

shows as No.5.

In Scheme 1, The synthetic route of poly(MMA-co-AEMA) was shown. The

reaction of 4-azidobenzoyl chloride with poly(MMA-co-HEMA) was carried out in the

presence of N,N,N-triethyl amine at 4 °C. For the ^{1}HNMR spectra (Fig 11), the

introduction of 4-azidobenzoyl group into HEMA moieties in poly(MMA-co-AEMA)

was confirmed by the appearance of resonance peaks at 4.32 and 4.55 ppm on ^{1}H NMR

spectrum, assignable to protons in ethylene group of HEMA moiety, and at 7.18 and

8.09 ppm, assignable to protons in 4-azidobenzoyl group. Amounts of 4-azidobenzoyl

group were determined by area ratio of peaks at 7.18 and 9.08 ppm to peaks at 3.87 and

4.15 ppm, assignable to unreacted methylene groups of HEMA moiety. [18,19]

Theoretically, if all of HEMA group react with 4-azidobenzoyl chloride, the

amounts of 4-azidobenzoyl group increased with HEMA fraction. However, just the

sample No.4 react completely, the mole ratios of MMA/HEMA was 8.6 : 1.0, the as

show in ^{1}H NMR spectra (Fig.11). For the table 3, No.1 to No.4, the amounts of

4-azidobenzoyl group increased with decreasing HEMA fraction in the

Poly(MMA--co-AEMA) from 1.03 to 0.59 mmol/g, with conversion percent from 100%

to 14%(Fig. 12).Yet, it was difficult for us to discuss the reason.

Table 2 Synthesis of Poly(MMA-*co*-HEMA)

	MMA	HEMA	AIBN	THF	$C_6H_{16}O_3SiS$	m:n Mn/10^3
No.1	3ml (28mmol)	1.36ml (11.2mmol)	1.6mg (0.17mmol)	20ml	60 (0.33mmol)	2/1 (11)
No.2	6ml (56mmol)	2.04ml (16.8mmol)	1.6mg (0.17mmol)	20ml	60 (0.33mmol)	4/1 (13)
No.3	6ml (56mmol)	1.36ml (11.2mmol)	1.6mg (0.17mmol)	20ml	60 (0.33mmol)	6/1 (15)
No.4	3ml (28mmol)	0.34ml (2.8mmol)	1.6mg (0.17mmol)	20ml	60 (0.33mmol)	8/1 (16)
No.5	12ml (128mmol)	0.68ml (5.6mmol)	1.6mg (0.17mmol)	20ml	60 (0.33mmol)	14/1 (24)
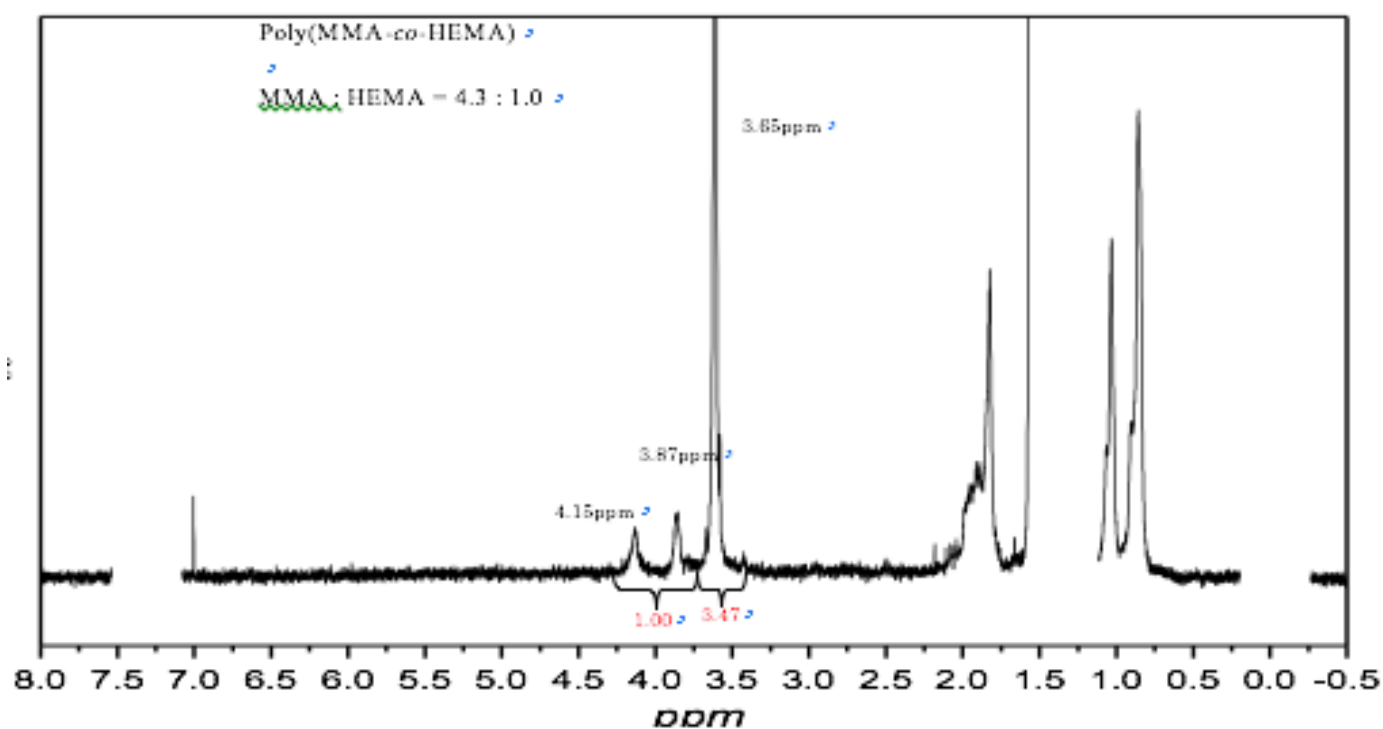
Figure 7 Typical 1H NMR spectra of poly(MMA-co-HEMA) with mole ratio of MMA/HEMA=4.3:1.0

Poly(MMA-*co*-HEMA)

MMA : HEMA = 6.5 : 1.0

3.65ppm

3.87ppm

4.15ppm

1.00   4.94
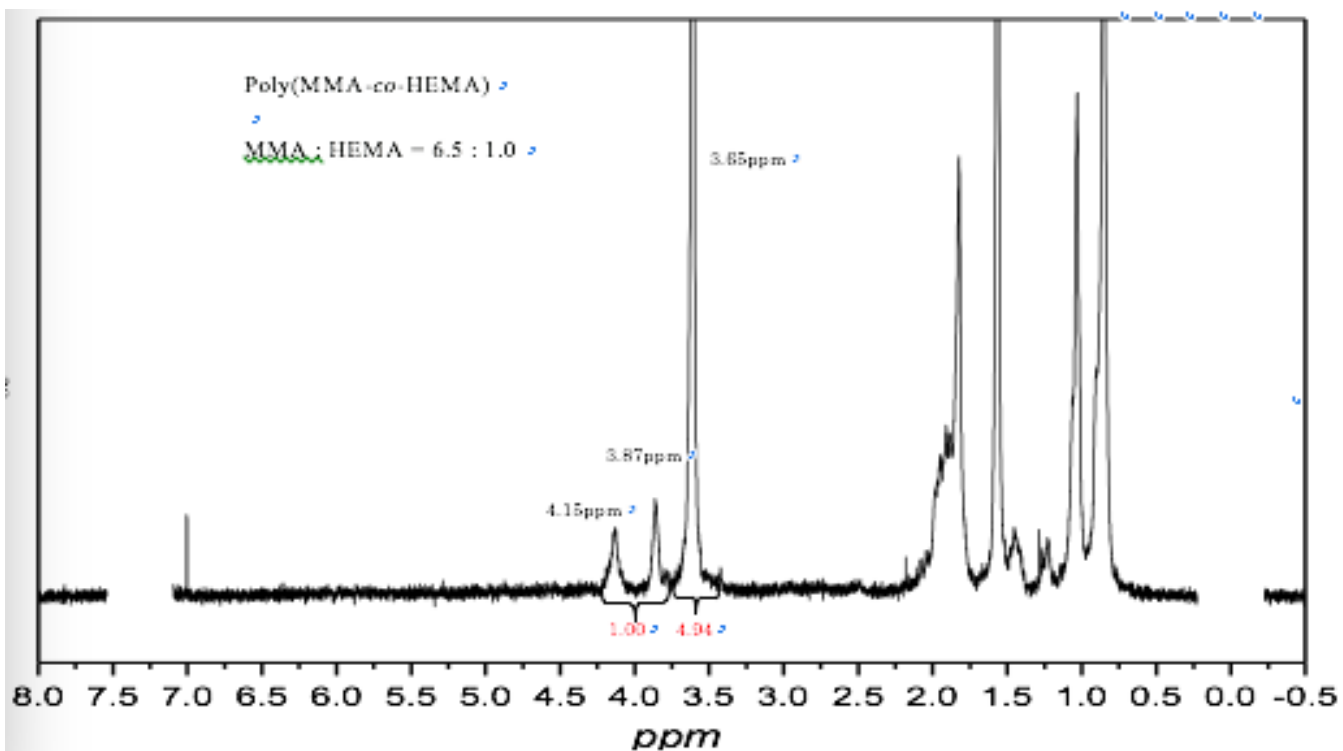
Figure 8 Typical 1H NMR spectra of poly(MMA-co-HEMA) with mole ratio of MMA/HEMA=6.5:1.0

Poly(MMA-*co*-HEMA)

MMA : HEMA = 9.3 : 1.0

3.65ppm

3.87ppm

4.15ppm

1.00   7.01
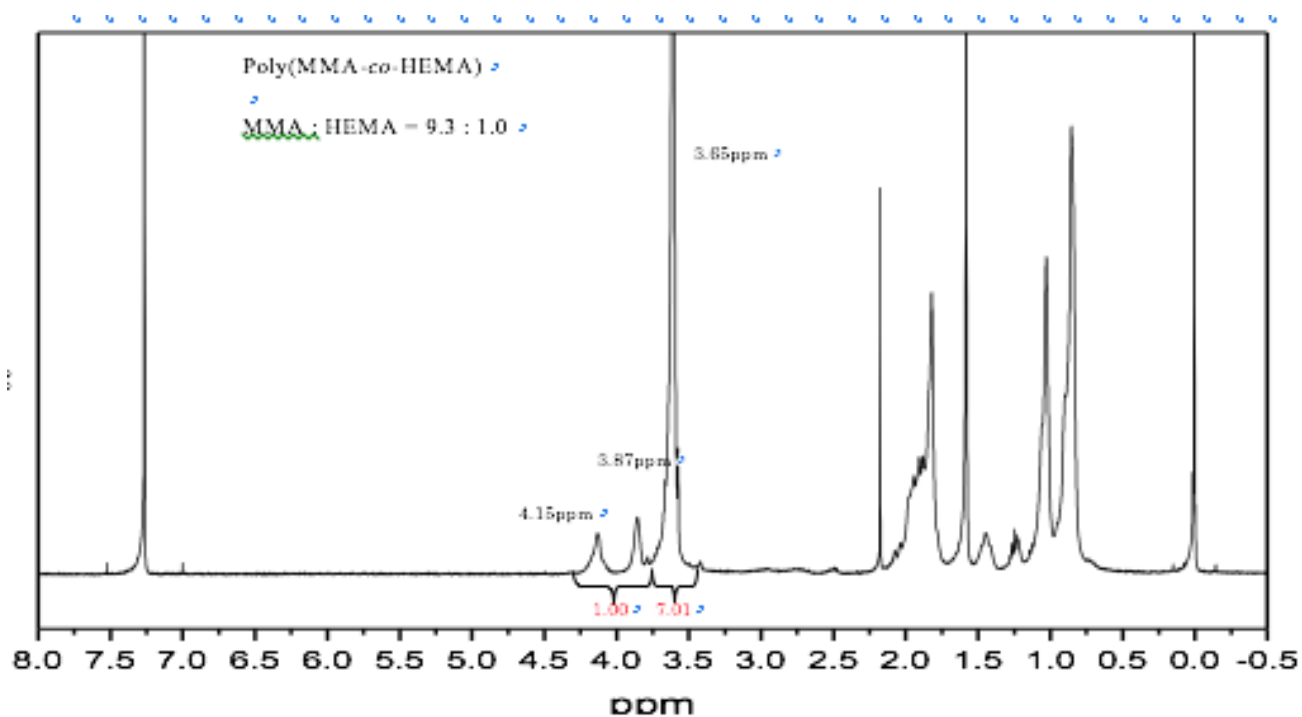
Figure 9 Typical 1H NMR spectra of poly(MMA-co-HEMA) with mole ratio of MMA/HEMA= 9.3:1.0

Poly(MMA-*co*-HEMA)

MMA : HEMA = 14.2 : 1.0

3.65ppm

3.87ppm

4.15ppm

1.00   10.86
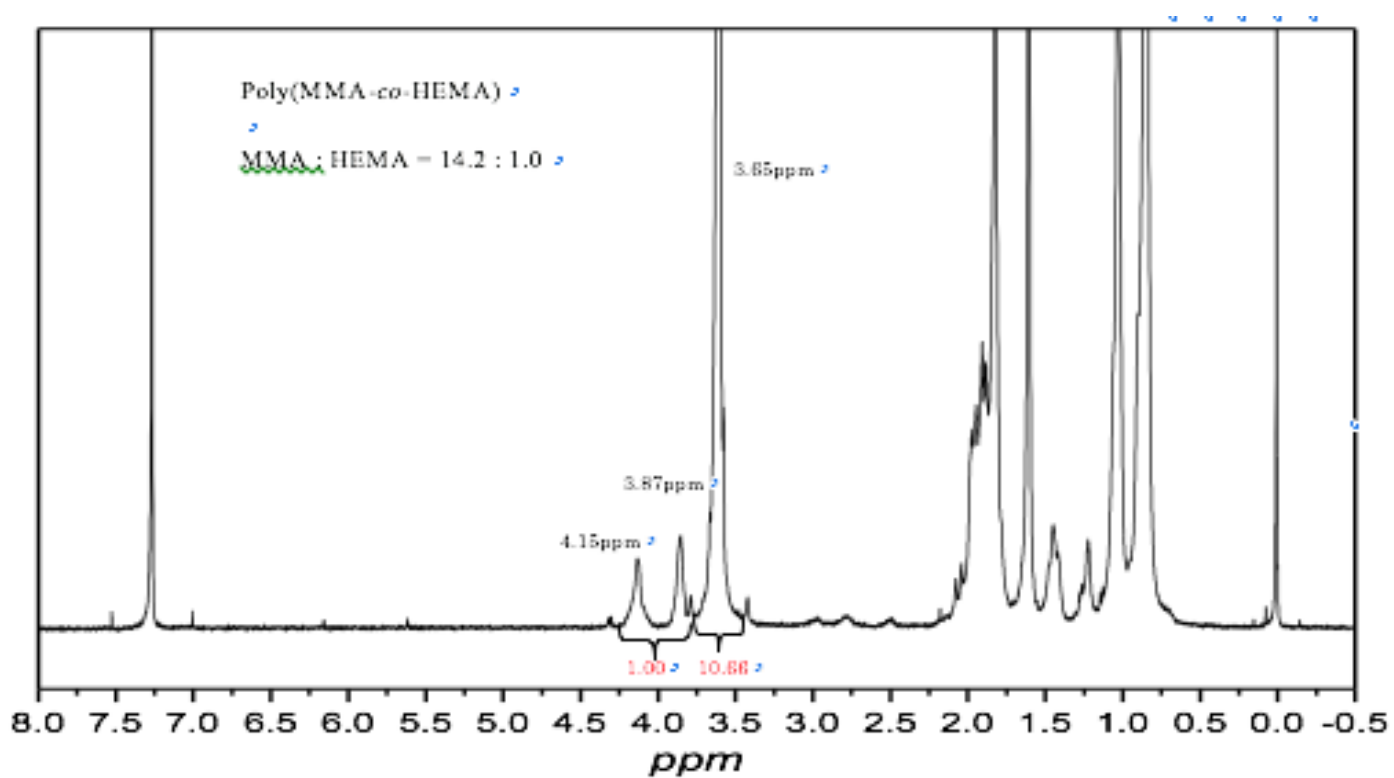
Figure 10 Typical 1H NMR spectra of poly(MMA-co-HEMA) with mole ratio of MMA/HEMA= 14.2:1.0

Probably there is favorable to react with Polymer chains of poly(MMA-*co*-AEMA) with high MMA fraction were probably favorable to react with 4- azidobenzoyl chloride due to highly affinity with chloroform. However, while the number-average molecular weight was24,000 (No.5), about twice as No.1 to No.4, the amounts of 4-azidobenzoyl group was decreased. Due to there is not enough samples with high the number-average molecular weight, so there is a difficult to for us to discuss the reasons here. Meanwhile, this result also suggested that there is a possible for us to control the target products via adjusting the ratios of HEMA to AEMA and the number -average molecular weight of polymer.

1.4　Conclusion

In summary, **chapter 1** has show that 4-azidobenzoyloxy groups introduced in poly(MMA-*co*-HEMA) [poly(methyl methacrylate-*co*-2-hydroxyethyl methacrylate)], synthesized by radical copolymerization, followed by esterification of 2-hydroxyethyl metharylate moieties with 4-azidobenzoyl chloride.

Gel permeation chromatography (GPC) measurements for poly(MMA-*co*-HEMA) show that the number-average molecular weight of polymers. The molecular weight distribution is narrow and unimodal, indicating that the polymerization was performed in a controlled manner.

After discuss the relationship between products and and reaction conditions, we found that the polymer chains of poly(MMA-*co*-AEMA) with high MMA fraction were probably favorable to react with 4- azidobenzoyl chloride due to highly affinity with chloroform. When the number-average molecular weight was high, it did not conform to this law. This result also suggested that there is a possible for us to control the target products via adjusting the ratios of HEMA to AEMA and the number

-average molecular weight of polymers.

Table 3 Synthesis of Poly(MMA-*co*-AEMA)

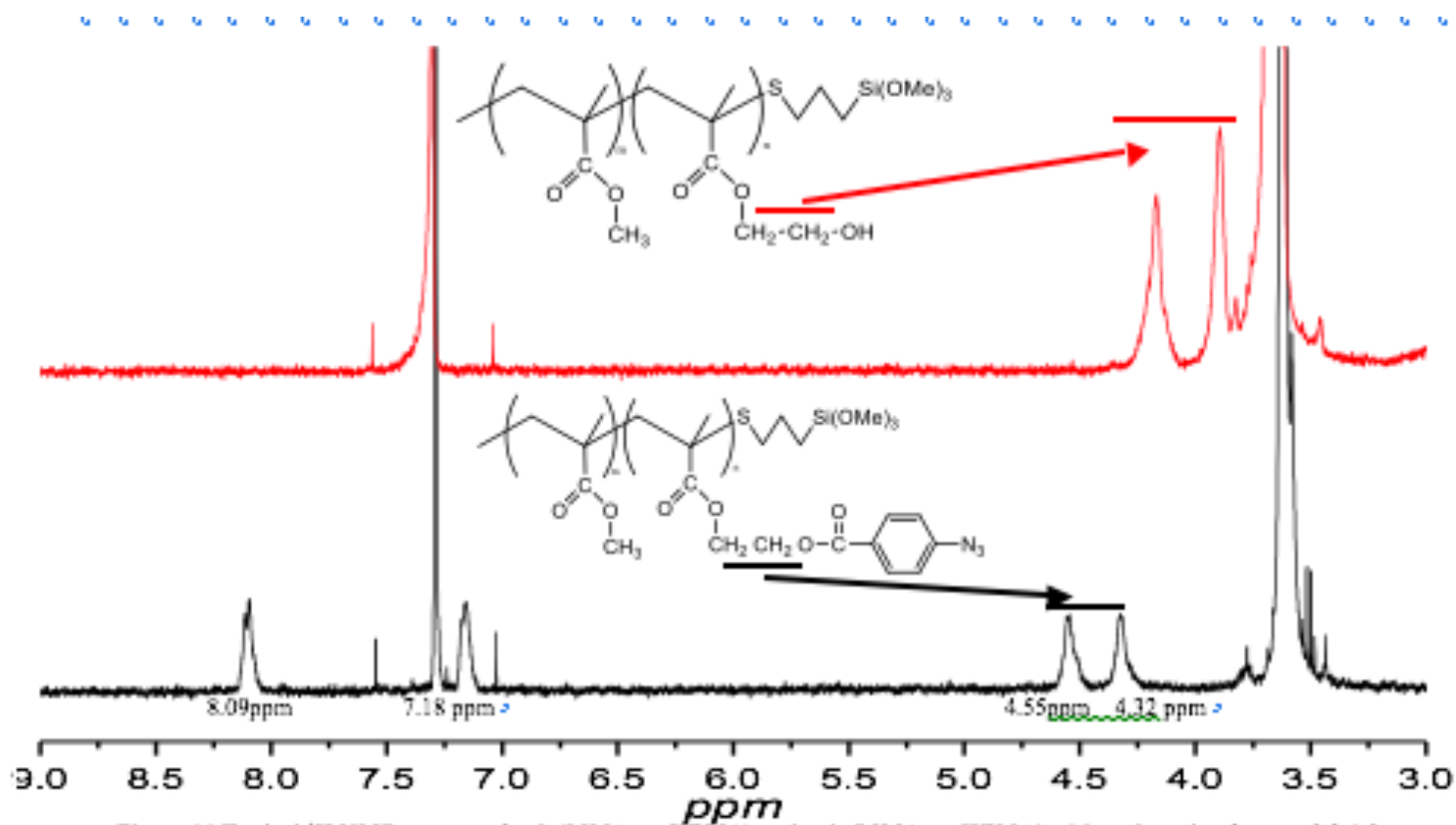| Polymer		$4\text{-}N_3C_6H_4$ group	Conversion
Mole ratio	Mn/10^3	(mmol/g)	Percent
	m/n		(%)
2/1	11	0.59	14
4/1	13	0.73	38
6/1	15	0.86	52
8/1	16	1.03	100
14/1	24	0.22	40

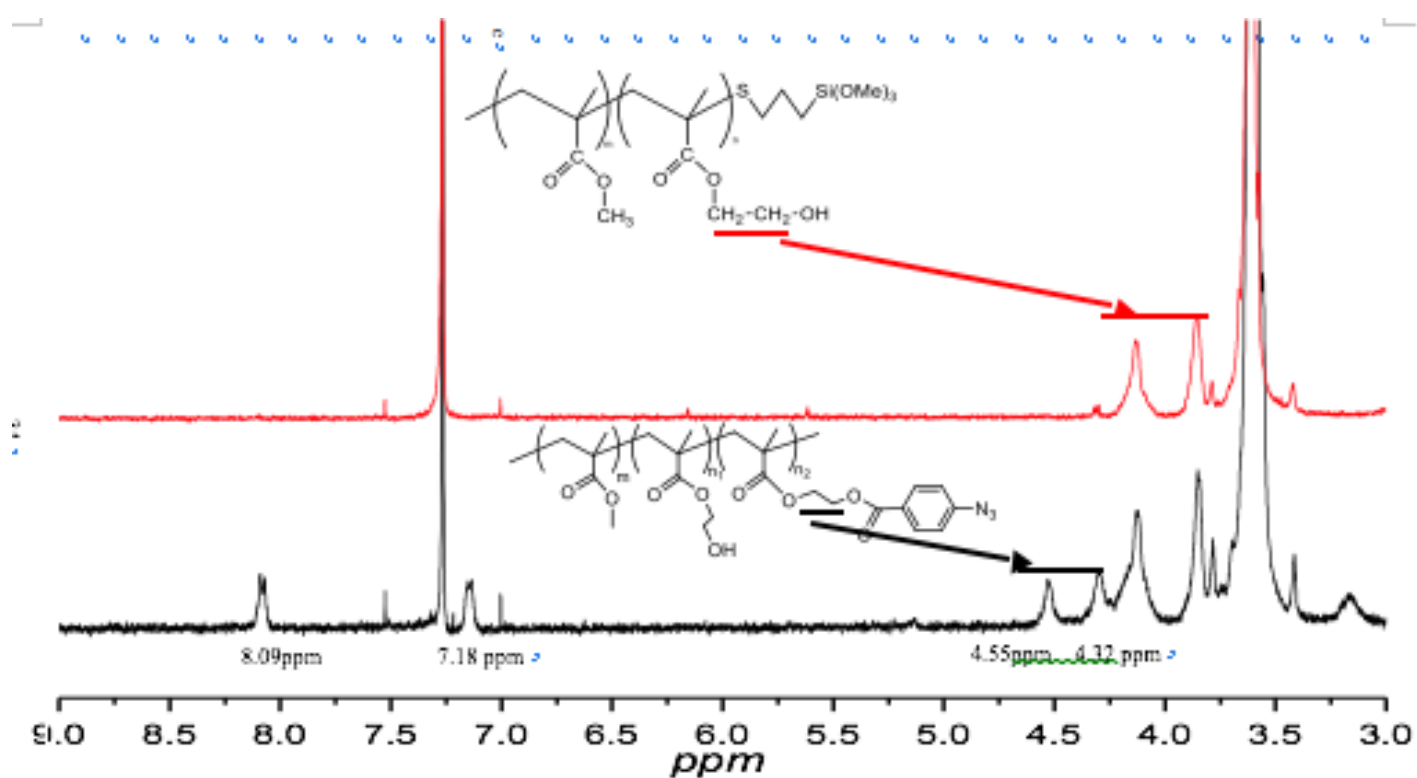Figure 11 Typical ¹H NMR spectra of poly(MMA-co-HEMA) and poly(MMA-co-HEMA) with mole ratio of m:n = 9.3:1.0

Figure 12 Typical ^{1}H NMR spectra of poly(MMA-co-HEMA) and poly(MMA-co-HEMA) with mole ratio of m:n = 6.5:1.0

35

References

1   Prucker, O.; Ruhe, J. *Macromolecules* **1998**, *31*, 592-601.

2   Tatsuro, G.; Tomohiro, K.; Madoka, T.; Toru, M.; Kazuhiko, I. *Biomaterial*. **2006**, 27, 5151-5160.

3   Ana C. C. E.; Lindsay, B.; Tito, T.; Krzysztof, M.; Ana Barros, T. *Nanocomposites,* **2007,** 7, 1230-1236.

4   Tsubokawa, N.; Machida, S.; Yoshikawa, S. *J. Polym. Sci., Polym. Chem.* **2002**, *36*, 3165-3172.

5   Yoshikawa, J.; Tsubokawa, N. *Polym. J.* **1996**, *28*, 317-322.

6   S.H. Wu, C.-Y. Mou and H.-P. Lin, *Chem. Soc. Rev.*, **2013**, 42,3862–3875.

7   Vinu, K. Z. Hossain and K. Ariga, J. Nanosci. *Nanotechnol.*, **2005**, 5, 347–371.

8   T. Hermanson, Bioconjgate Techniques, *Academic Press,* **1996**.

9   Yang, S. Gaib and J. Lin,Chem. *Soc. Rev.*, **2012**, 41, 3679–3698.

10 Paul D.D., Lauren F., Molly S.S. *Biomaterials*. **2002**, 23, 3843-3851.

11 Yasemin Y.D., Volkan C., Levent A.D. *Macromolecules*, **2009**, 42, 3743-3749.

12 Yu, Z.; Hong Qun, L.; Nian Bing, L. *Bioprocess Biosyst Eng,* **2011,** 34, 215-221.

13 Bourgeat-Lami, E.; Tissot, I.; Lefebvre, F. *Macromolecules,* **2002**, 35, 6185-6191.

14 Lei, X.; Hongbo, L.; Rumin, W.; Liang, C. *J Polym Res,* **2011**, 18, 1017-1021.

15 Yasemin, Y.D.; Volkan, K.; A.Levent, D.; Naciye, T.; Yusuf, Y. *Macromolecules*, **2009**, 42, 3743-3749.

16 Lan, J.; Ping, L.; Jianhua, H.; Changchun, W. *Polym Int,* **2004**, 53, 142-148.

17 Durairaj, B.; John, R.D.; Jimmy, W.M.: Mattthew, S.B. *Macromol. Rapid Commun*. **2005**, 26, 481-486.

18 Ana, S.S; David, A.F.; Jose, A.P. *Chem. Commun.*, **2014**, 50, 1871-1874.

19 Lorea, B.; Jose, A.P. *Polymers* **2011**, *3*, 1673-1683.

Chapter 2

Preparation of C_{60}-tethered
Polymer grafted silica (C_{60}/polymer/SiO$_2$)

2.1 Introduction

Fullerene has received much interest for applications in smart and functional

materials owing to its characteristic properties, such as electron-accepting or -releasing

capacity, high refractive index, high heat conductivity and absorption in the UV region.

So far, a number of papers have reported fundamental and practical studies employing

modified or unmodified fullerenes in applications such as solar cell devices, fillers and

semiconductors.[1–4] In most cases, a surface modification of fullerenes was performed to

promote dispersion or to increase the solubility of the fullerenes in solution.[5] However,

surface modification by a covalent bond sometimes spoils the innate properties of

fullerene. Furthermore, the addition of surfactants causes fullerene to leak from the

final products and contaminate the environment. We have reported a polymer

dispersant, poly(methyl methacrylate-*co*-2-naphthyl methacrylate)

(poly(MMA-NMA)), effectively disperses fullerene in an organic solvent without

spoiling the original properties of fullerene.[6]

Silica is widely used as a raw material in many applications, including paints, fillers

of plastics, carriers of catalysts, supports in heterogeneous organic synthesis and

stationary phase of chromatography, owing to its non-toxicity, stability and availability.

A recent development in colloid chemistry also made it possible to control the size of

the colloidal inorganic particles ranging from nanometer to micrometer size.[7]

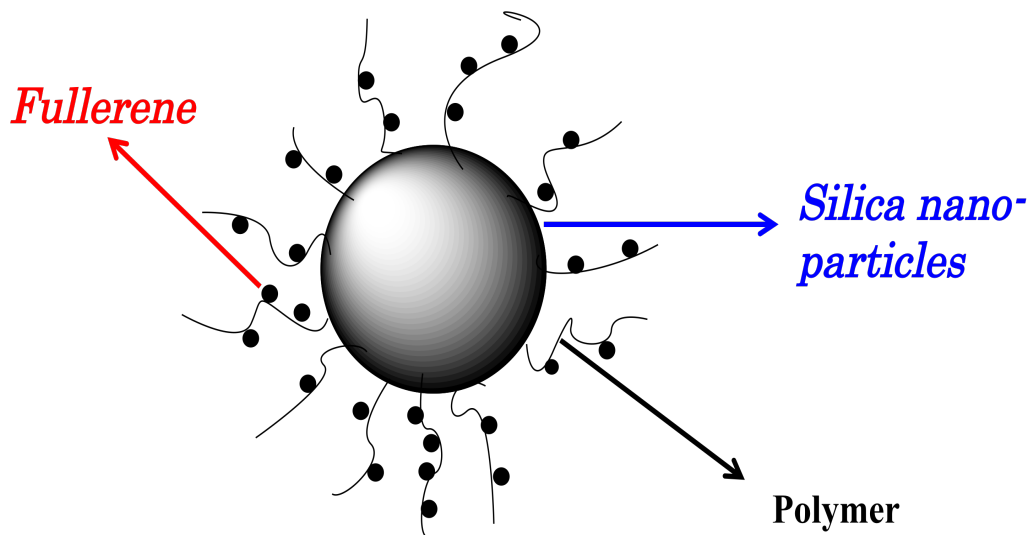Nanometer-sized colloidal silica is an especially attractive material

Fig. 13 Preparation of C$_{60}$-tethered polymer-grafted silica(C$_{60}$/polymer/SiO$_2$)

owing to its spherical shape, colorlessness and high stability in an aqueous solution. An

aqueous solution containing colloidal silica <20nm is usually transparent. Therefore,

polymer composites consisting of fairly well-dispersed fullerene and silica

nano-particles can result in the fabrication of unique functional materials, that is,

silica-reinforced and heat-conductive transparent composites.

At present, almost of these composite nano-structure are synthesized via blend be

conjugated with surface groups, or post-synthesis surface groups which are exhibited

many reports, and they showed broad application prospect.[8-15]

In **Chapter 2**, we showed that synthesis of fullerene (C_{60})-tethered polymer grafted

silica and colloidal crystallization of the particles was investigated. (Fig. 13)The

particles were prepared by the reaction of C_{60} with 4-azidobenzoyl groups introduced in

poly(methyl methacrylate-*co*-2-hydroxyethyl methacrylate). The reaction afforded

bindings of C_{60} in the range from 0.44×10^4 to 1.71×10^4 molecules/particle. The C_{60}

amounts did not monotonously increase with 4-azidobenzoyl group on the particles, but

decreased with mole fraction of methyl methacrylate in the copolymer.

2.2 Experimental Section

2.2.1   Materials

Colloidal silica aqueous sol, containing 20wt% SiO_2 of 134 nmin diameter with a

polydispersity 0.030, was kindly gifted by   Nikki Catalysts & Chemical Co. Ltd.,

Kanagawa, Japan.Fullerene (C_{60}), Nanom purple ST, was purchased from Frontier

Carbon Co. Ltd., Tokyo,   Japan.tetrahydrofuran (THF), diethyl ether, 1,2-dimethoxy

ethane (DME),   toluene were obtained from   Wako Chemicals Co. Ltd., Osaka, Japan

2.2.2   Preparation of poly(methyl methacrylate-*co*-2-(4-azidobenzoyloxy)ethyl

metharylate)-grafted silica

Colloidal silica suspended in ethanol was prepared by solvent exchanging with azeotropic evaporation of water after addition of ethanol to the original aqueous sol. A mixture of 0.5 g Poly(MMA-*co*-AEMA), 50 mL colloidal silica ethanol suspension, containing1.0 g SiO_2, and 50 mL DME was put into a 100-mL flask. After sonication for 30 m, the suspension was stirred at 90 °C for 5 h along with azeotropical removal of ethanol. Centrifugal washing with THF eight times and drying under reduced pressure gave 1.0 g Poly(MMA-*co*-AEMA)/SiO_2, with 47.8 mg/g grafted polymer. ^{13}C CP/MAS NMR: 10.3–25.2 (broad, −CH2− C(CH3)(C=O)−), –CH2–C(CH3)(C=O)–), 44.5 (–CH2− C(CH3)(C=O)−), 40.8–62.0 (broad, O–CH3, O–CH2CH2–O), and 177.8 ppm (C=O).

2.2.3 Reaction of C_{60} with poly(methyl methacrylate-*co*-2-(4-azidobenzoyloxy) ethyl metharylate)-grafted silica

Into 20 mL toluene, 50 mg C_{60} and 1.0 g Poly(MMA-*co*-AEMA)/SiO_2 were put, and the mixture was stirred at 110 °C under a nitrogen atmosphere for 24 h. Centrifugal separation of resulting particles with toluene and drying under reduced pressure gave 0.88 g 4. ^{13}C CP/MAS NMR: 9.9–26.8 (broad, –CH2– C(CH3)(C=O)–), –CH2–C(CH3)(C=O)–), 44.6 (–CH2–C(CH3)(C=O)–) , 39.1–70.3 (broad, O–CH3, O–CH2CH2–O), 107.7–153.0 (broad, –C60), and 177.3 ppm (C=O).

2.2.4 Characterization

Amounts of grafted polymer on poly(MMA-*co*-AEMA)/SiO_2 and C_{60}-tethered poly(MMA-*co*-AEMA)/SiO_2 were determined by weight decrease (Wpolymer) during

C₆₀

Scheme 2 the synthetic route of C$_{60}$-tethered poly(MMA-*co*-AEMA)/SiO$_2$.

Poly(MMA-*co*-AEMA)   Poly(MMA-*co*-AEMA)/SiO$_2$

Fullerene-poly(MMA-*co*-AEMA)/SiO$_2$

42

9   8   7   6   8 7b 9 6   5   4   2   3
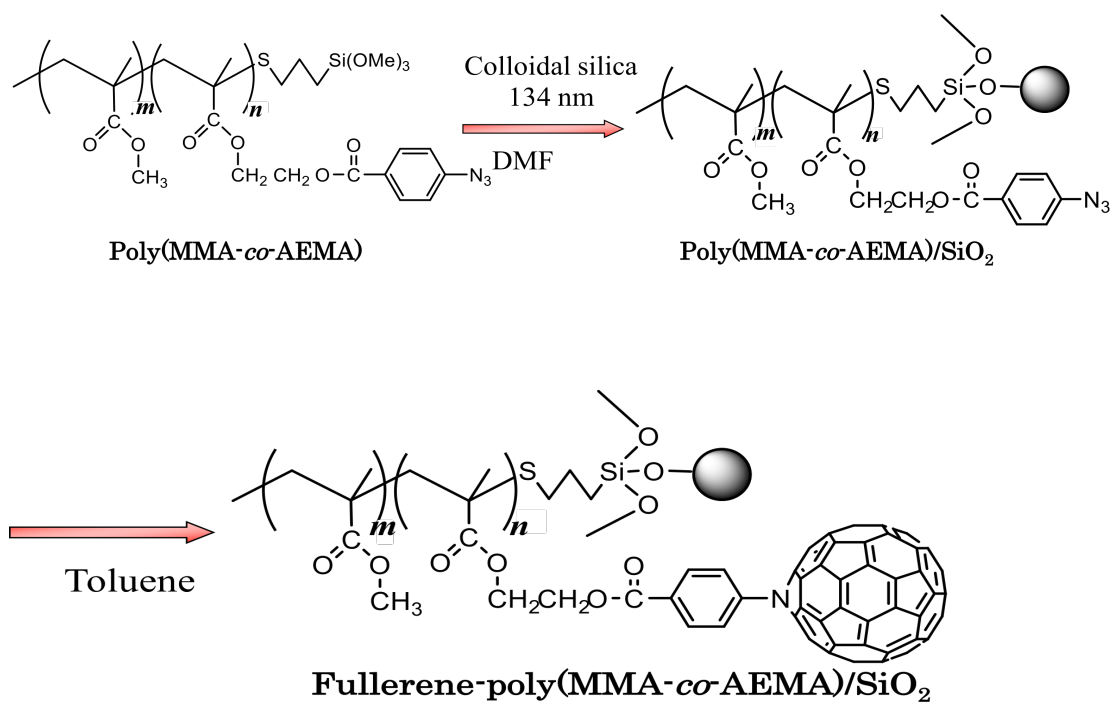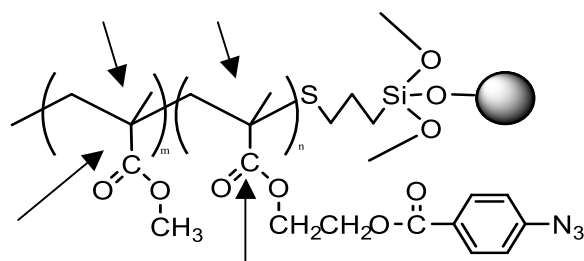
δ (ppm)	Assignment
145.1-149.3	**2**
107.3	**3**
177.4	**4,9**
44.4	**5**
39.7	**6**
9.9-27.6	**7,8**

Table 4 ^{13}C NMR chemical shifts of poly(MMA-*co*-AEMA)-grafted silica

Fig. 14 ^{13}C CP/MAS NMR spectra of Poly(MMA-*co*-AEMA) grafted with SiO$_2$
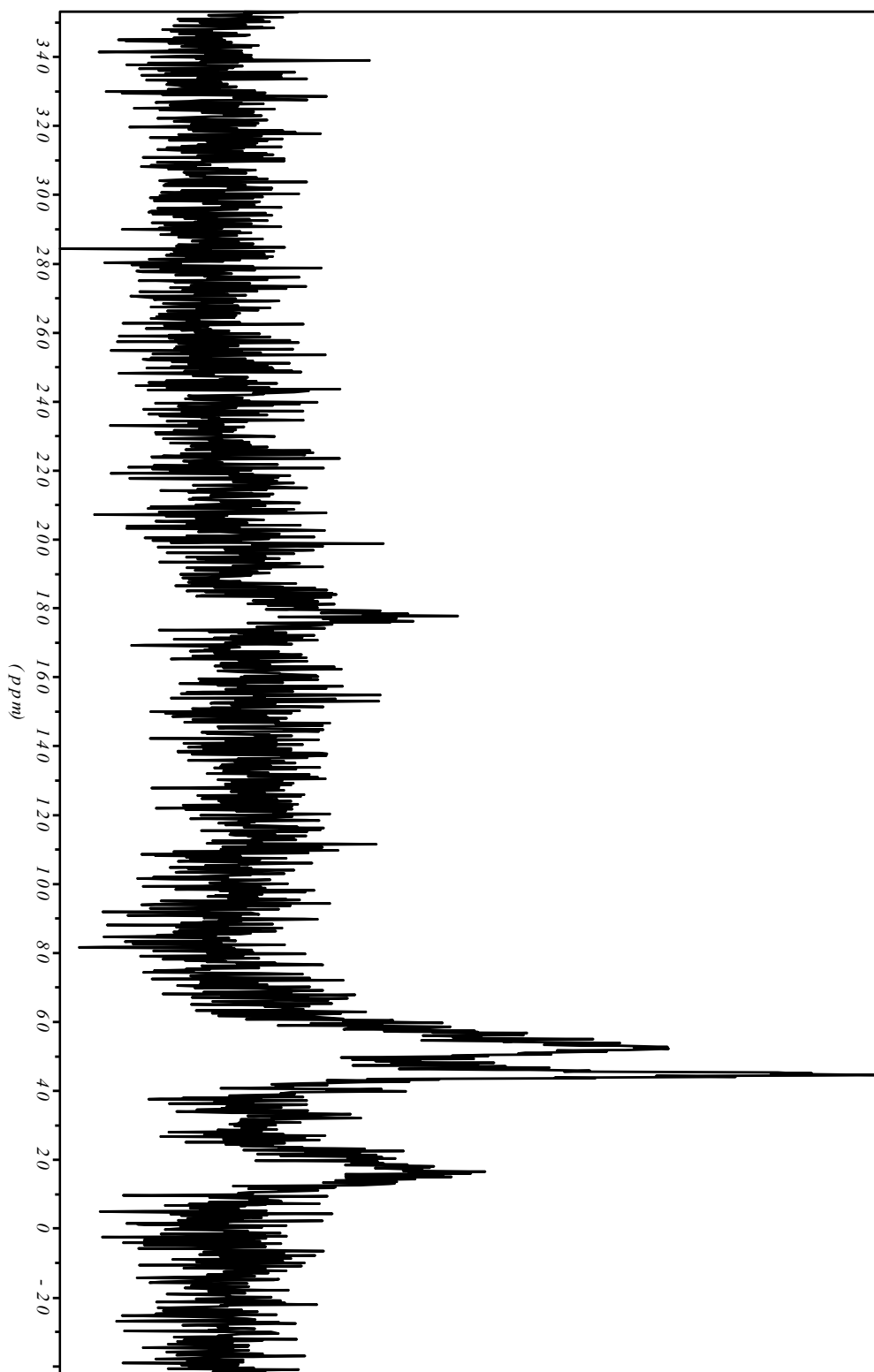
elevation from 170 to 420 °C on a thermogravimetric analysis. The amount of C_{60}

tethered on 4 was also determined by weight loss (Wc_{60}), corresponding to C_{60} ignition,

44

during elevation from 550 to 800 °C. ^{13}C CP/MAS NMR spectra for solid state samples were recorded on a Bruker AVANCE 300 (300 MHz) using a 7-mm rotor prove, Karisruhe, Germany respectively.

2.3 Result and discussion

We synthesized the poly(MMA-*co*-AEMA) in the chapter 1.In this **chapter 2**, Poly(MMA-*co*-AEMA) was reacted with silica nano-particles and C_{60}, respectively In Scheme 2, the synthetic route of C_{60}-tethered poly(MMA-*co*-AEMA)/SiO_2 was shown.

In order to determinate conveniently the grafted polymer and C_{60} on silica. We give priority to reaction with silica nano-particles. A mixture of poly(MMA-*co*-AEMA), colloidal silica ethanol suspension and DME was put into a flask, after sonication for 30min. the suspension was stirred at 90^OC for 1day with azetropical remove of ethanol, Centrifugal washing with THF six times and drying under reduced pressure.

For ^{13}C CP/MAS NMR spectra of Poly(MMA-*co*-AEMA) grafted with SiO_2 (Fig. 14) ,it was distinctly indicate that Poly(MMA-*co*-AEMA) graft on silica nano-particles by the appearance of resonance peak at $9.9 \sim 27.6ppm$, $39.7ppm$, $44.4\ ppm$, $107.3ppm$, $177.4ppm$ and $145.1 \sim 149.3ppm$ (Table 4).However, for ^{13}C CP/MAS NMR spectra just could qualitative analysis, quantitative analysis for determinate the graft polymer on silica should via other determination method.

TGA (Thermal Gravimetric Analysis) is a useful procedure for the characterization of the organic grafting process. This technique allows the study of interaction strength between the attached organic groups and the surface with increasing temperature.
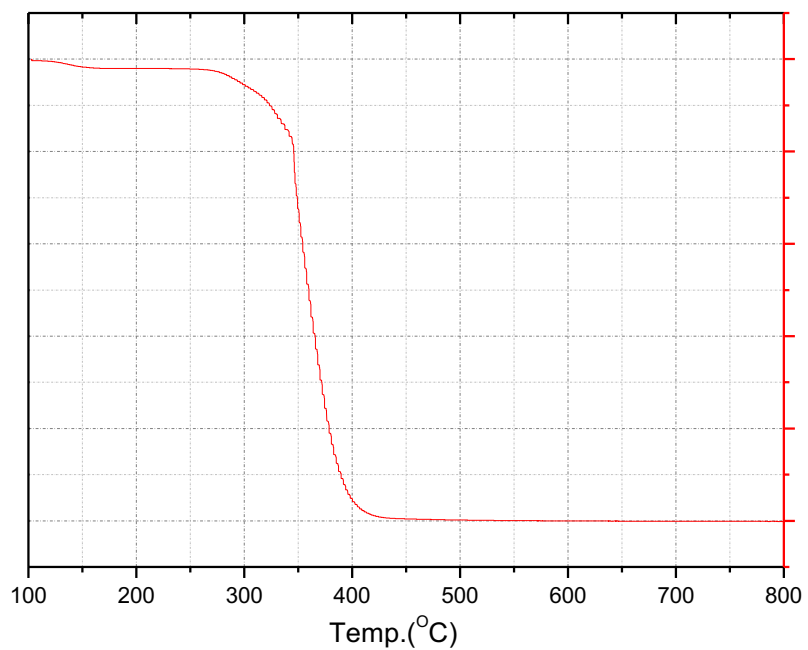
Fig. 15 Typical thermo gravimetic thermogram of poly(MMA-*co*-HEMA)
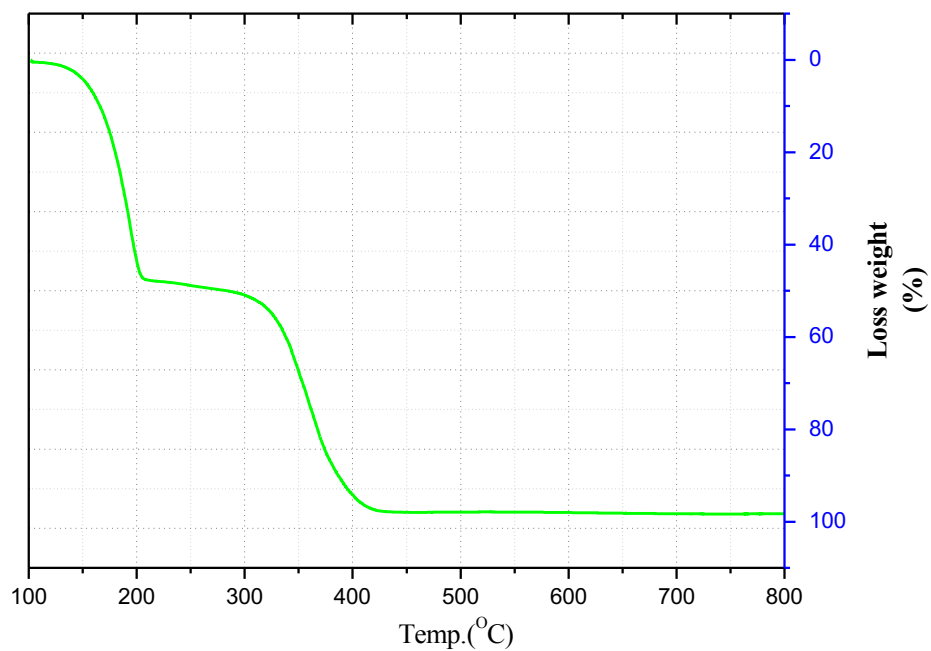

Fig. 16 Typical thermo gravimetic thermogram of poly(MMA-*co*-AEMA)

Previous thermal analysis reports have shown that the molecular dynamics of the

polymer and the silica glass, typically of 10 ~ 15 nm pore size, affect the glass transition temperature of the polymer.

The adsorbed amounts were measured using thermal gravimetric analysis (TGA) unzipping after initial cleavage of head-to-head linkages and AEMA moiety, reached with a TGA 2950 (TA Instruments, New Castle, DE). Samples of approximately 10 ~15 mg were placed in the sample tray and heated from an ambient temperature to 800 °C at a rate of 1°C/min. Nitrogen was used as purge gas at 50 mL/min.

As shown in Fig. 15, sample weight loss during the thermal degradation of poly(MMA-*co*-HEMA) occurred in three distinct steps. The first step, attributed to unzipping after initial cleavage of head-to-head linkages, reaches a maximum weight loss rate at 120°C and resulted in -2% total weight loss.

The second step, attributed to initial scission at vinylidene chain ends followed by unzipping, reached in the ranged from 270°C to 350°C and was characterized by a -10% sample weight loss.

The third degradation step, due to unzipping after random chain cleavage, reached a maximum weight loss at 420°C, resulting in the decomposition of the remaining polymer.

As shown in Fig. 16, sample weight loss during the thermal degradation of poly(MMA-*co*-AEMA) occurred in three distinct steps. The first step, attributed to Fig. 8in the ranged from 120°C to 205°C and was characterized by a -10% sample weight loss.

The second step, attributed to initial scission at vinylidene chain ends followed by unzipping, reached in the ranged from 270°C to 350°C and was characterized by a -10% sample weight loss.

The third degradation step, due to unzipping after random chain cleavage, reached

a maximum weight loss at 420°C, resulting in the decomposition of the remaining polymer.

As shown in Fig. 17, sample weight loss during the thermal degradation of poly(MMA-*co*-AEMA) graft with silica occurred in four distinct steps. The first step, attributed to unzipping after initial cleavage of head-to-head linkages and AEMA moiety, reached in the ranged from 120°C to 205°C and was characterized by a -1% sample weigh

The second step, attributed to initial scission at vinylidene chain ends followed by unzipping, reached in the ranged from 250°C to 300°C and was characterized by a -1% sample weight loss.

The third degradation step, due to unzipping after random chain cleavage, reached in the ranged from 300°C to 420°C, and was characterized by a -4% sample weight loss.

The forth degradation step, due to unzipping after the polymer were absorbed into the silica surface chain cleavage, reached in the ranged from 490°C to 540°C, resulting in the decomposition of the remaining polymer.

For the table 5, the amounts of poly(MMA-*co*-AEMA) on silica as show from 50.0 to 51.8 mg/g-SiO$_2$(NO.1~No.4),In the case of high number-average molecular weight, the amounts of poly(MMA-*co*-AEMA) on silica was 57.8 mg/g-SiO$_2$, it was ndicated that the amounts of polymer almost similar.(Table 5)

For this result, the amount of polymer on silica did not depend on the ratio of MMA to AEMA, but increased with the increase of high number-average molecular weight. It was implied that the number of polymer grafted on silica surface have a limit.
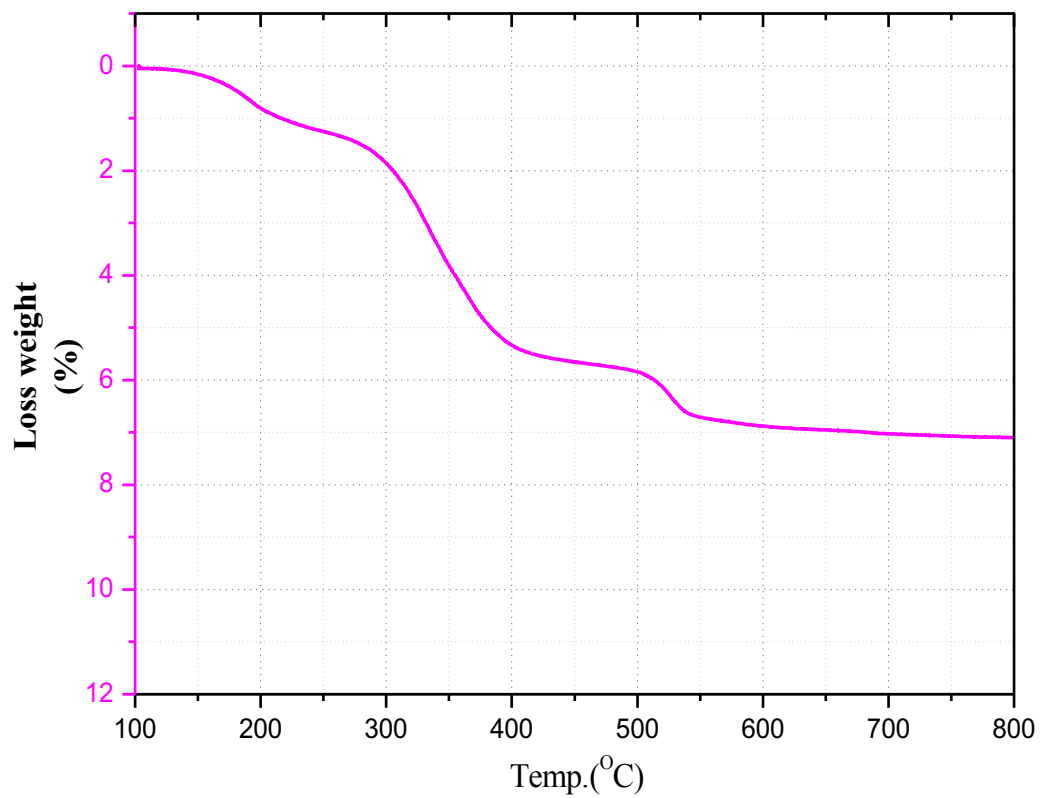
Fig. 17 Typical thermo gravimetic thermogram of

poly(MMA-*co*-AEMA) grafted with silica

Table 5 Synthesis of Poly(MMA-*co*-AEMA)/SiO$_2$

Polymer		Grafted polymer on SiO$_2$ / mg/g-SiO$_2$	4-N$_3$C$_6$H$_4$ group on SiO$_2$ /μmol/ g-SiO$_2$
M$_n$/10^3	m/n		
2/1	11	51.8	34.1
4/1	13	50.5	36.9
6/1	15	49.1	41.1
9/1	16	50.0	51.5
14/1	24	57.8	10.5

.

Into toluene, fullerene and polymer grafted silica were put, and the mixture was stirred at 110°C under a nitrogen atmosphere for 24h. Centrifugal separation of resulting particles with toluene and drying under reduced pressure. For ^{13}C CP/MAS I NMR spectra of C_{60}-tethered Poly(MMA-*co*-AEMA) grafted with SiO_2(Fig. 18) ,it was distinctly indicate that C_{60} tethered on Poly(MMA-*co*-AEMA) grafted with SiO_2 nano-particles by the appearance of resonance peak at 120.5~142.7ppm.(Table 6) Likewise, quantitative analysis for determinate the tethered C_{60} on Poly(MMA-*co*-AEMA) via Thermal Gravimetric Analysis (TGA).

We studied powered samples in nitrogen atmospheres at a flow rate of 50 mL/min subsequent treatment of C_{60} to 800°C under nitrogen at heating rate of 1°C/min. As shown in Fig. 19, sample weight loss during the thermal degradation of C_{60} occurred in two distinct steps.

The first step, attributed to demonstrates loss of a volatile component, reached in the ranged from 300°C to 540°C, was characterized by a 3-5% sample weight loss. The second step, attributed to unzipping delocalized π bond of C_{60}, reached in the ranged from 550°C to 750°C , and resulting in the decomposition of the remaining $C_{60.}$

As shown in Fig. 20, sample weight loss during the thermal degradation of C_{60} tethered poly(MMA-*co*-AEMA) graft with silica occurred in five distinct steps.

The first step, attributed to unzipping after initial cleavage of head-to-head linkages and AEMA moiety, reached in the ranged from 120°C to 205°C and was characterized by a -1% sample weigh The second step, attributed to initial scission at vinylidene chain ends followed by unzipping, reached in the ranged from 250°C to 300°C and was characterized by a -1% sample weight loss. The third degradation step, due to unzipping after random chain cleavage, reached in the ranged from 300°C to

9　δ　7　6　8⁷　9⁶　5　4　2　3　　1

δ (ppm)	Assignment
120.5-142.7	**1**
145.1-149.3	**2**
107.3	**3**
177.4	**4,9**
44.4	**5**
39.7	**6**
9.9-27.6	**7,8**

Table 6 ¹³C NMR chemical shifts of poly(MMA-*co*-AEMA)-grafted silica

Fig. 18 ^{13}C CP/MAS NMR spectra of Poly(MMA-*co*-AEMA) grafted with SiO$_2$
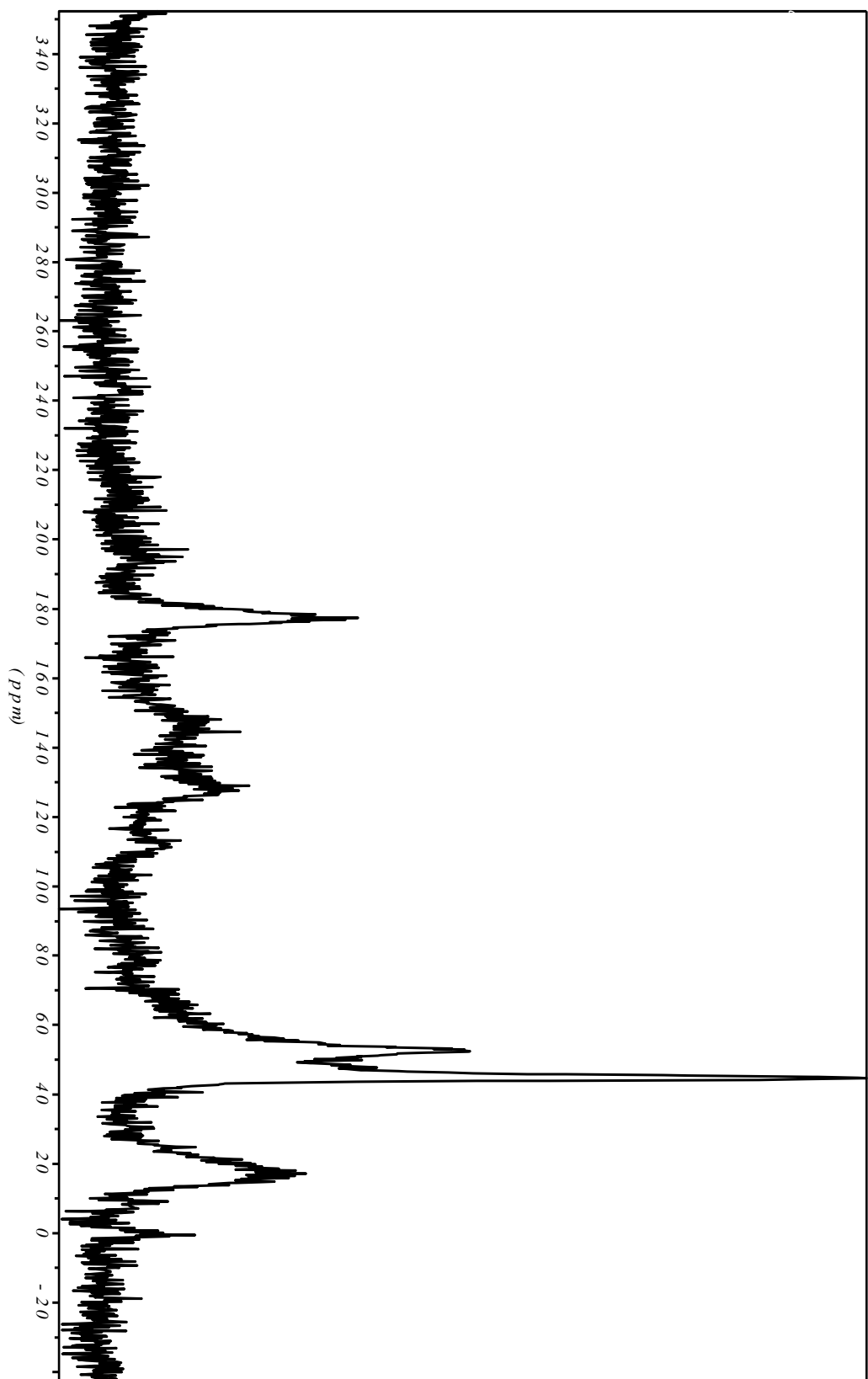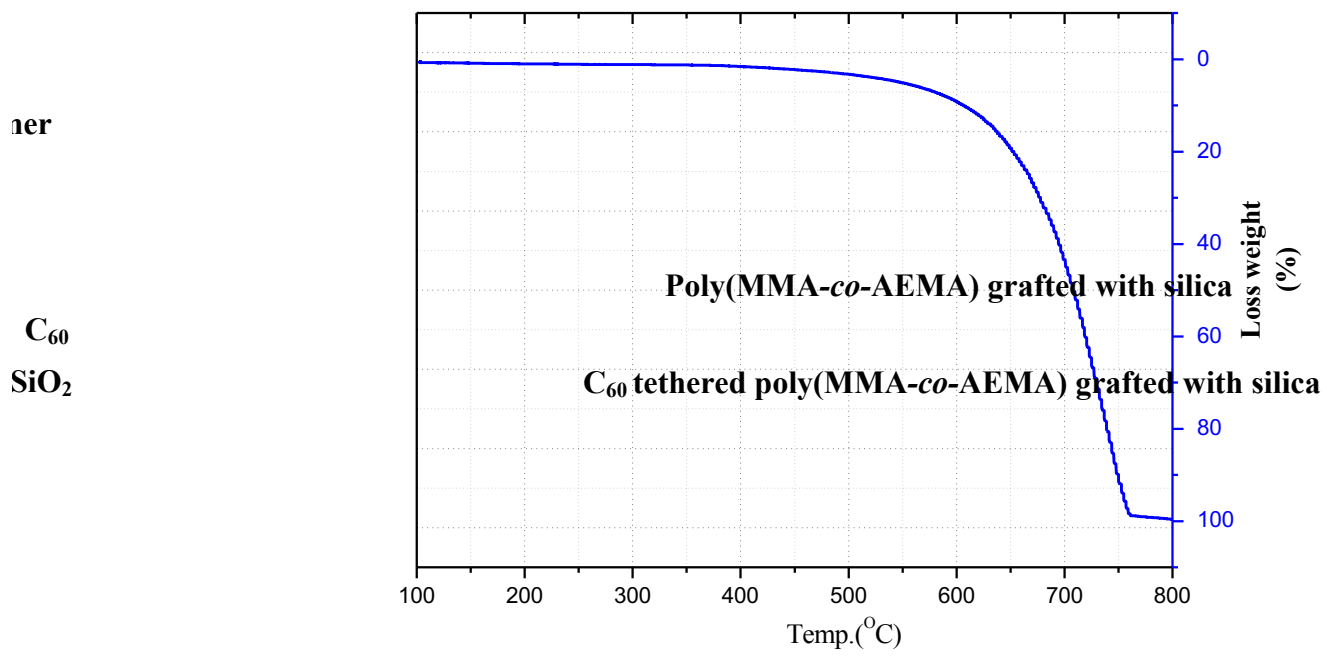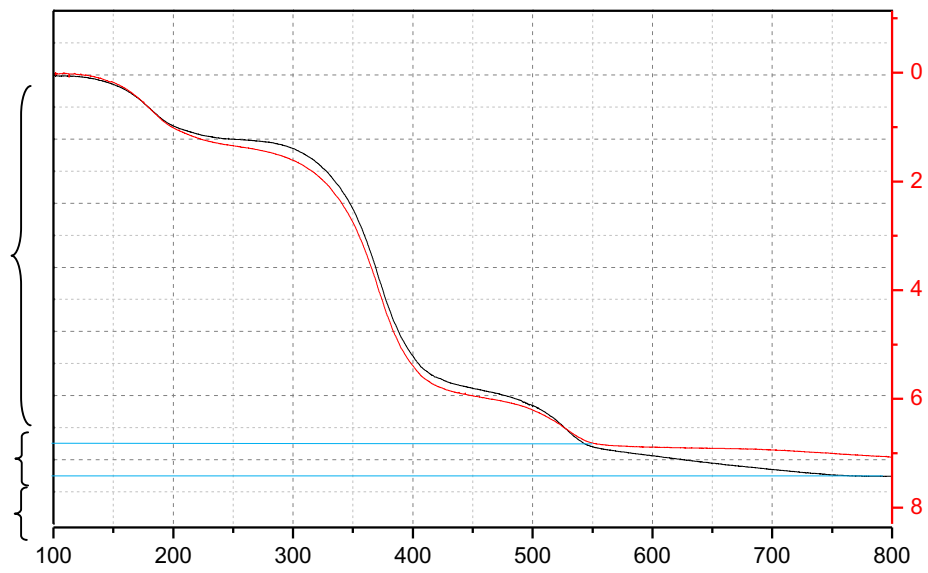
Fig. **19 Typical thermo gravimetic thermogram of C₆₀**

Fig. 20 Ty**pical thermo gravimetic thermogram of poly(MMA-*co*-AEMA) grafted**

with silica and C₆₀ tethered poly(MMA-*co*-AEMA) grafted with silica

54

420°C, and was characterized by a -4% sample weight loss.The forth degradation step, due to unzipping after the polymer were absorbed into the silica surface chain cleavage, reached in the ranged from 490°C to 540°C, resulting in the decomposition of the remaining polymer. The fifth degradation step, attributed to unzipping delocalized π bond of C_{60}, reached in the ranged from 550°C to 750°C, resulting in the decomposition of C_{60}.

For the table 5, the amounts of C_{60} on poly(MMA-*co*-AEMA) grafted with silica as show from 1.90 to 7.37 mg/g-SiO2, that is, from 2.63 to 10.2 μmol/g-SiO$_2$. Interestingly, amounts of tethered C_{60} decreased with mole ratio of MMA/HEMA in poly(MMA-*co*-HEMA), not simply with amounts of 4-azidobenzoyl group on poly(MMA-*co*-AEMA) grafted with silica. Probably, polymer chains with 4-azidobenzoyl groups on poly(MMA-*co*-AEMA) grafted with silica, prepared from high mole fraction of HEMA in poly(MMA-*co*-HEMA), might have high flexibility during the reaction of C_{60} with poly(MMA-*co*-AEMA) grafted with silica in toluene. In other words, 4- azidobenzoyl group in grafted polymer composed of high mole fraction of MMA moiety on poly(MMA-*co*-AEMA) grafted with silica could be less active for C_{60} bindings due to shrinking of polymer chains in toluene.

2.4 Conclusion

In summary, **chapter 2** has show that the amounts of poly(MMA-*co*- AEMA) on silica as show from 50.0 to 51.8 mg/g-SiO$_2$(NO.1~No.4). In the case of high number-average molecular weight, the amounts of poly(MMA-*co*-AEMA) on silica was 57.8 mg/g-SiO$_2$, it was indicated that the amounts of polymer almost similar. Unexpected, the amount of polymer on silica did not depend on the ratio of MMA to AEMA, but increased with the increase of high number-average molecular weight.

Table 7 The amounts of C_{60} on poly(MMA-*co*-AEMA) grafted with silica

Polymer		$4\text{-}N_3C_6H_4$ group in polymer / mmol/g	Grafted polymer on SiO_2 / mg/g-SiO_2	$4\text{-}N_3C_6H_4$ group on SiO_2 /μmol/ g-SiO_2	C_{60} on product mg/g-SiO_2 μmol/g-SiO_2	
$M_n/10^3$	m/n					
2/1	11	0.59	51.8	34.1	7.374	10.24
4/1	13	0.73	50.5	36.9	5.647	7.84
6/1	15	0.98	49.1	41.1	3.746	5.20
9/1	16	1.03	50.0	51.5	2.934	4.01
14/1	24	0.22	57.8	10.5	1.896	2.63

It was implied that the number of polymer grafted on silica surface have a limit. The amounts of C_{60} on poly(MMA-*co*-AEMA) grafted with silica as show from 1.90 to 7.37 mg/g-SiO$_2$, that is, from 2.63 to 10.2 μmol/g-SiO$_2$.Therefore,we guess that 4-azidobenzoyl group in grafted polymer composed of high mole fraction of MMA moiety on poly(MMA-*co*-AEMA) grafted with silica could be less active for C_{60} bindings due to shrinking of polymer chains in toluene.

References

1   Fukuzumi,S. & Kojima, T. Photo. *J. Matr. Chem*.**2008**, 18, 1427–1439.

2   Mateo-Alonso, A., Guldi, D. M., Paolussi, F. & Prato, M. *Angew. Chem. Int. Ed,***2007**, 46, 8120–8126.

3   Li, Y. *Acc. Chem. Res.***2012,**45, 723-733.

4   Patnaik, A. *J. NaonoSci. Nanotechnol,***2007**, 7, 1111-1150.

5   Ravi, P., Dai, S., Wang, C. & Tam, K. C. *J. Nanosci. Nanotechnol,* 2007,7, 1176-1196.

6   Yoshinaga, K., Motokucho, S., Kojio, K. & Nakai, A. *Colloid Polym. Sci.* **2012**,290, 1221–1226.

7   Gieshe, M. & Osseo-Asare, K. *(ed. Sugimoto, T.) ch*. **2000**, 126–189.

8   *M*asayoshi, A., Norifumi, F., Masashito, S. and Seiji, S. *J. Mater. Chem.* **2003**, 13, 2145-2149.

9   Davydenko, M.O., Radchenko, E.O.,Yashchuk, V.M., Dmitruk, I.M., Matishevska, O.P., Golub, A.A. *J. Mol. Liq.* **2006,** 127, 145-147.

10 Elena, V.B., Vladimir, A.B., Vladimir, P.S., Vitaliy, G.G., *Carbon,* **2003,** 41, 2339-2346.

11 Hemei, C., Dawei, Q., Chunhui, D., Penyuan, Y. and Xianmin, Z. *Proteomics,* **2009,**

9, 380-387.

12 Kailoon, C., Menchem, E. *Environ. Sci. Technol.* **2008,** *42,* 7607–7614.

13 Sudeep, P.K., Binil ltty ipe, K., Georege, T. and George, M.V. *Nano Lett.* **2002,** 2, 29-35.

14 Arihiro, T., Tishihir, N., Masatomi, O., Shoji, E. and Kazukiyo, K. *Tetrahedron Lett.* **1998,** 39, 9031-9034.

15 David, J.H., Evan, E., and Irene, T. *J. Phys. Chem. B* **2006,** *110,* 15963-15972

Chapter 3

Colloidal crystallization of the C_{60} tethered poly(MMA-*co*-AEMA) grafted with silica particles in organic solvent

3.1 Introduction

Three-dimensional (3D) particle arrays structure, inter-sphere distance of which is comparable to visible light wave length, has been receiving much attention for promising application to optical devices, such as wave guide, sensor, and so on .[1-6] So far, many approaches for fabrication of 3D particle arrays have been reported .[1-22]One of promising approaches is the fabrication employing colloidal crystals formed in solution, due to easy tuning inter-sphere space by changing the volume fraction and to exhibiting sharp and clear Bragg reflection. In most of cases, the fabrications have been carried out by using colloidal crystals formed in aqueous solution and immobilized in hydrogels.[7,10.14-18] However, in the practical application, it is quite difficult to utilize the hydrogels for optical devices, because of containing much water fraction. In this respect, we have successfully achieved colloidal crystallization of polymer-grafted silica in organic solvents[23-26] and then immobilization in polymer matrix[19-22]. Colloidal crystallizations in organic solvents are favorable for fabrication of 3D particle-arrayed structure by immobilization in polymer matrixes because of being able to utilize various polymerization reactions.

Concerning colloidal crystallization in solution, in many cases, monodisperse colloidal silica, polystyrene, and poly(methyl methacrylate) are employed for colloidal particles because of giving stable crystallites. Among them, colloidal silica usually brings stable colloidal crystals in aqueous solution due to negatively high
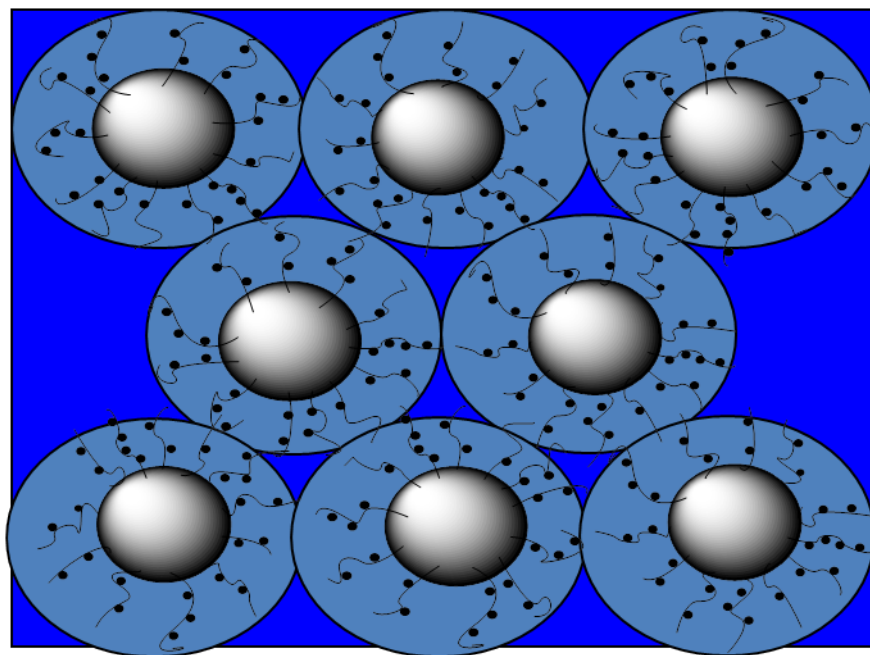
Fig. **21Colloidal crystallization of the C$_{60}$ tethered poly(MMA-*co*-AEMA)**

grafted with silica particles in organic solvent

surface charge. However, fabrication of 3D particle-arrayed optical device from colloidal crystals of silica has major shortcomings stemming from original property of silica, comparatively low refractive index, and dielectric constant. In this respect, we have reported that introduction of ferrocenyl groups in polymer grafted onto silica particles effectively increases refractive index of colloidal crystal system.[27]

Meanwhile, fullerenes have been attractive and highlighted materials due to spherical π-conjugated molecule exhibiting characteristic properties, i.e., electron accepting or releasing abilities, high dielectric constant, high heat conductivity, thermal stability, high refractive index, radical trapping, UV absorption, and so on. Thus, C_{60} and C_{60}-based nanomaterials have been contributing to a variety of promising application to functional materials, such as high surface area particles and supports in catalysis [28], electron carriers in electronic devices[29], and semiconductors [30,31]. Furthermore, Tu and coworkers have recently reported that grafting of C_{60} into polyesters elevates refractive index to give the maximum value of 1.79 [32]. Therefore, incorporation of C_{60} into colloidal crystals could lead not only to improvement of refractive index but also to challenging fabrication of new functional materials, exhibiting specific properties of C_{60}.

In this **chapter 3,** preparation of C_{60}-tethering polymer-grafted silica and colloidal crystallization in organic solvent were investigated (Fig. 21). Critical volume fraction and reflection spectra were evaluated. Inter-sphere distances in the colloidal crystals mostly agreed with calculated values on assumption of fcc-closed packing. Therefore, it was suggested that the crystallization occurred due to electrostatic repulsion between the particles as well as those of colloidal silica particles in aqueous solution.

3.2 Experimental

3.2.1 Characterization of particle size distribution

Particle size and its distribution were determined by a dynamic light scattering (DLS) on an Otsuka Electronics DLS-7000 spectrophotometer, equipped with a He–Ne laser (10 mW, 633 nm), Osaka, Japan. Reflection spectra of colloidal crystals were recorded on a multichannel spectrometer, Hamamatsu Photonics PMA-11, Shizuoka, Japan.

3.2.2 Colloidal crystallization

The C_{60}-tethered polymer-grafted silica (C_{60}/polymer/SiO_2) particles were dispersed in acetonitrile. After ultrasonic-wave irradiation, the suspension was kept at room temperature. The formation of colloidal crystals was confirmed by iridescence caused by Bragg diffraction from the particle array with constant intervals. The inter-particle distance and the size of single crystals were determined by reflection spectroscopy.

3.2.3 Critical volume fraction (ϕ_0)

In centrifuge tube, the C_{60}-tethered polymer-grafted silica (C_{60}/polymer/SiO_2) particles were put and dispersed in acetonitrile. After ultrasonic-wave irradiation, the suspension was centrifuged, reject the supernatant. Then, add the acetonitrile dropwise, and ultrasonic-wave irradiation. The colloidal crystals were observed, after sit for a moment. When the colloidal crystals could not were observed, the solvent was measured by suction pipet. ϕ_0(Fig.22) was presented by the following equation: X (g / ml) was weight of the composite in 1ml

$$\Phi < \Phi_0 \qquad \Phi_0 \qquad \Phi_0 < \Phi$$
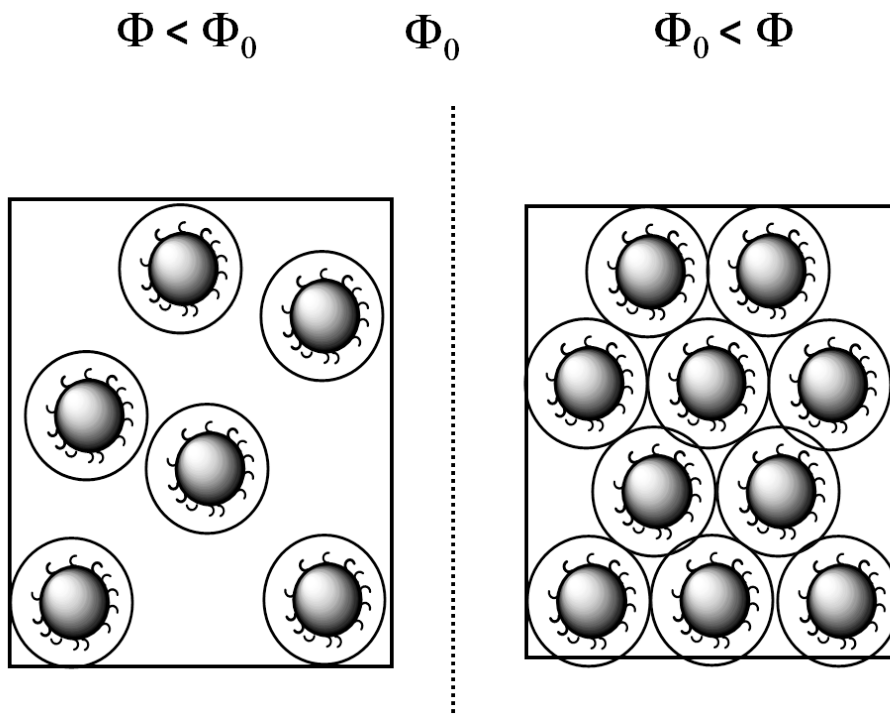
Fig.22 Critical volume fraction(Φ_0) : Minimal volume fraction of silica in colloidal crystallization .

X (g /ml) = weight of the composite (g)/ volume of solvent was measured by suction

$a_{calcd} = 0.9047 \times 1 - \phi$

pipet (ml)

Y (mg/ gSiO$_2$) was the amount of polymer grafted with silica, Z (g/ml) was the amount of polymer of X (g /ml)

Z(g / ml) = X (g / ml)×Y / 1000 (g / gSiO$_2$)

W(g / ml) was weight of silica nano-particles in X (g / ml)

W (g / ml) = X (g / ml) − Z (g / ml)

The proportion of silica was 2.2(g / ml) and polymer was 1.0 (g / ml), Φ_0 was presented by the following equation:

ϕ_0 = W(g / ml) ÷ 2.2 (g / ml) + Z (g / ml) ÷ 1.0 (g / ml)

3.2.4 Observation of colloidal crystallization and determination

The reflection spectra were measured at the 90° position from the cell surface by a multichannel spectral analyzer,PMA-11(Hamamatsu Photonics Co. Ltd., Hamamatsu, Japan), with a 150-W halogen lamp.

Colloidal crystallization of silica composite particles in organic solvent was observed by naked eyes and a digital camera.(Fig. 23)   Inter-sphere distance (d_{cal}) in colloidal crystal was calculated from the volume fraction on assumption of face centered cubic (fcc) closed packing by Eq. (1) ,

(1)

Where ϕ is volume fraction of polymer-grafted silica, d_{calcd} is neighboring inter-sphere distance and r is diameter of the particle.   The Inter-sphere distance (d_{obs}) in the crystals was also determined according to Bragg formula by following equation :

$$d_{obs} = \sqrt{\frac{3}{8}} \frac{\lambda_p}{n}$$ (2)

Halogen
Lump

Spectro
meter

$$d = (3/8)^{0.5} \frac{\lambda}{n_{sol}}$$

$$d = 4.198 \times r \times (\phi \times 100)^{(1)/3} \quad \dots (4)$$

r : Diameter of a silica particle / nm
d : Interparticle distance / nm
ϕ : Volume fraction
n_{sol} : Refractive index
λ : Peak wavelength / nm
(incident angle; 0°)

$$n_{sol} = n_{silica}\phi + n(1-\phi)$$

Fig. 24. Face centered cubic model.

Fig. 23. Reflection spectrum measuring
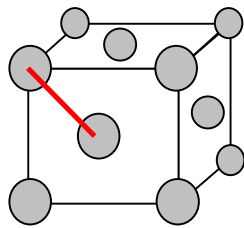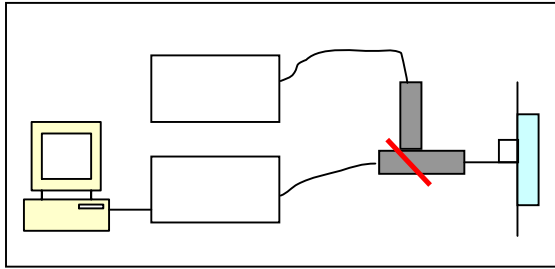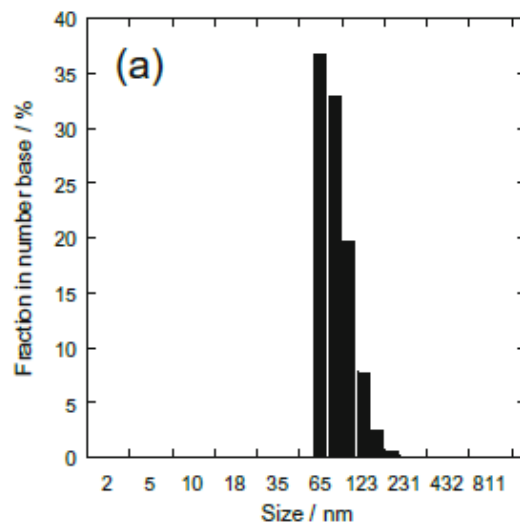
Fig..**25 Particle size distributions of original colloidal silica**
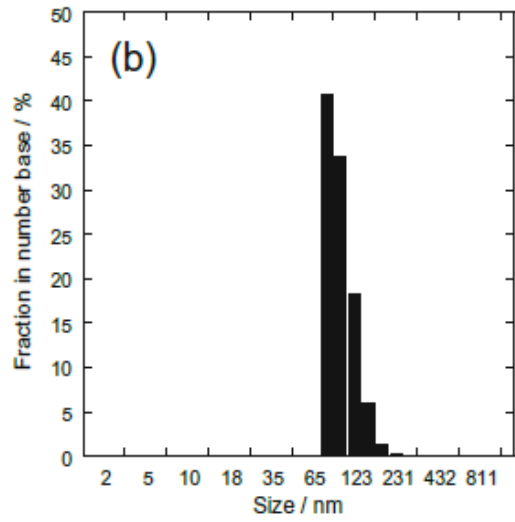
26a
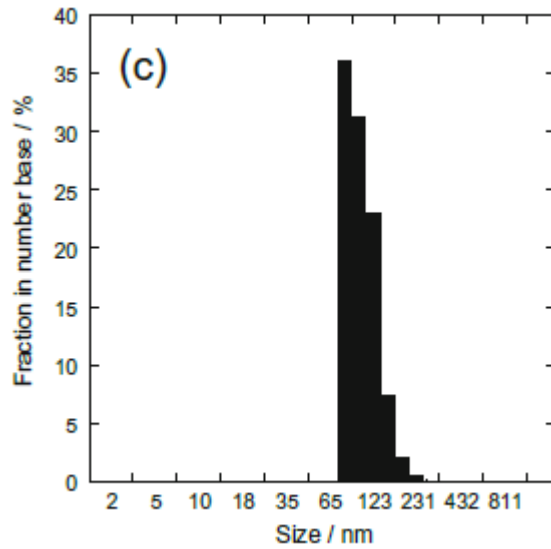
26b

Fig.26 Particle size distributions of Poly(MMA-*co*-AEMA)/SiO$_2$ (26a)

and C$_{60/}$ Poly(MMA-*co*-AEMA)/SiO$_2$(26b)

Where λ_p is the peak top wavelength on a reflection spectrum, n is average refractive

index of the suspension system calculated by Eq. (3)

$$n = \phi \times n_{silica} + (1 - \phi) \times n_{sol} \qquad (3)$$

Where, n_{silica} and n_{sol} are refractive index of silica and solvent, respectively, and ϕ is volume fraction of silica.(Fig. 24)

3.3 Result and discuss

Dynamic light scattering (also known as photon correlation spectroscopy or quasi-elastic light scattering) is a technique in physics that can be used to determine the size distribution profile of small particles in suspension or polymers in solution. It can also be used to probe the behavior of complex fluids such as concentrated polymer solutions. DLS was used characterize size of various particles including proteins, polymer, micells, carbohydrates, and nano-particles. If the system is mon o disperse, the mean effective diameter of the particles can be determined. This measurement depends on the size of the particles core, the size of surface structures, particles concentration, and the type of ions in the medium.

  We examined the particle size and particle size distribution of the silica nano-particles, poly(MMA-*co*-AEMA) grafted with silica nano-particles and C_{60} tethered poly(MMA-*co*-AEMA) grafted with silica nano-particles by DLS. For the results Fig. 25, the average particle sizes of SiO_2 was 134nm, poly(MMA-*co*- AEMA) grafted with silica nano-particles were in therange from 145 to 150 nm, being 11~16nm large than that of the original silica. The particles size slightly became larger by polymer grafting, but distributions of size were still narrow (Fig. 26a). Herefore, we confirmed that aggregation between the particles no occurred during the reaction of poly(MMA-*co*- AEMA) with silica nano-particles.

68

2:1 Φ = *0.147*
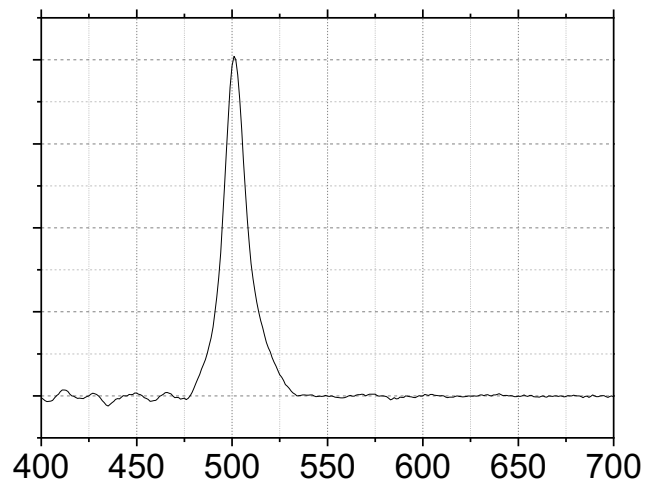
Fig. 27 Typical photographs and reflection spectra of the crystal(ϕ =0.147)

4: 1 Φ = *0.136*
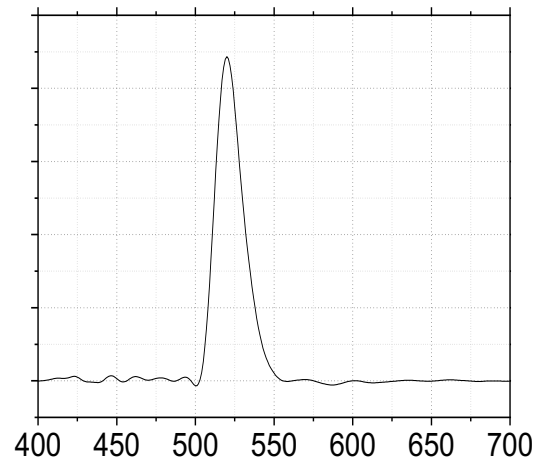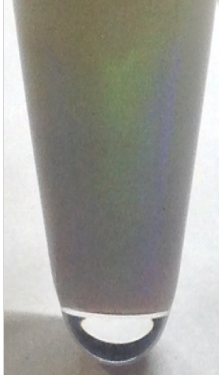
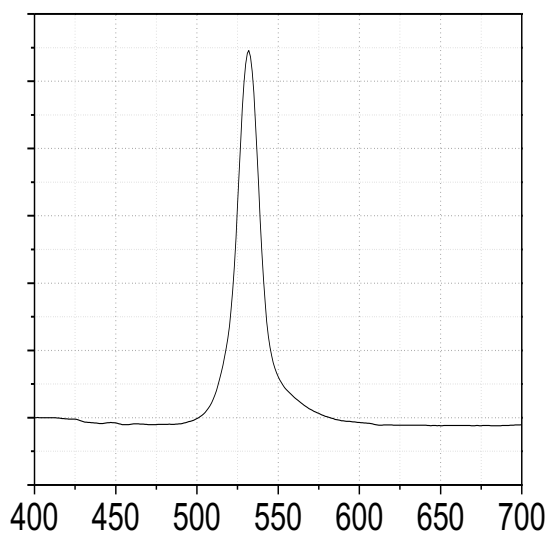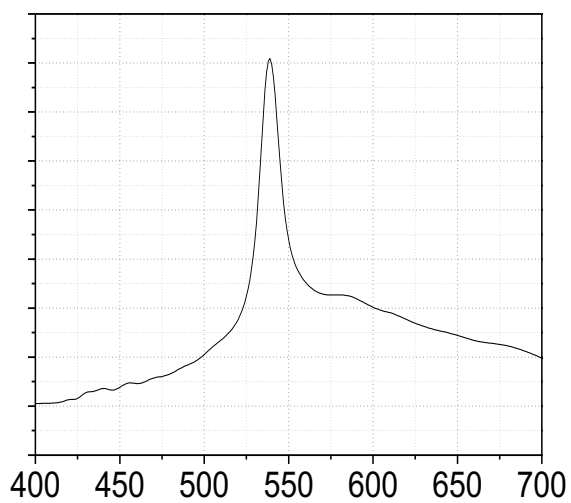**6: 1 Φ = *0.122***
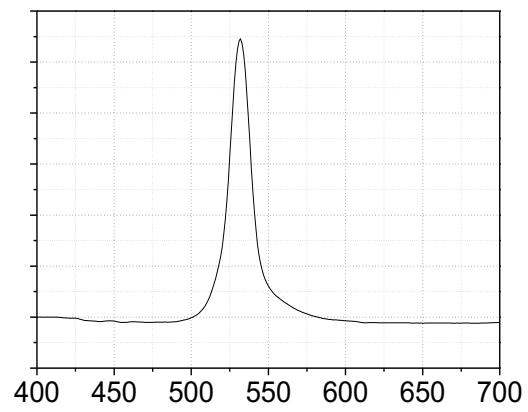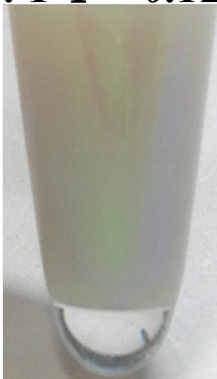
Fig. 28 Typical photographs and reflection spectra

of the crystals(ϕ=0.136and ϕ=0.122)

8: 1 Φ = *0.114*

14: 1 Φ = *0.106*

Fig. 29 Typical photographs and reflection spectra

of the crystals(ϕ=0.114 and ϕ=0.106)

The particles size of C_{60} tethered poly(MMA-*co*-AEMA) grafted with silica were

157~162nm being ca.12nm larger than those of poly(MMA-*co*-AEMA) grafted with silica, However those distribution were still narrow(Fig. 26b). Thus, It was observed that aggregation between particle of poly(MMA-*co*-AEMA) grafted with silica scarcely took place during the reaction of poly(MMA-*co*-AEMA) grafted with silica with C_{60}.

The authors have reported that poly(methyl methacrylate)- grafted silica particles formed colloidal crystals in polar solvents, such as CH_3CN, acetone, and N,N-dimethylformamide. When spheres of C_{60} tethered poly(MMA-*co*-AEMA) grafted with silica nano-particles were dispersed in CH_3CN formation of colloidal crystals was observed. Typical photographs and reflection spectra of the crystals were shown in Fig. 27. Color of the crystals of C_{60} tethered poly(MMA-*co*-AEMA) grafted with silica nano-particles with much amount of tethered C_{60} was dark green, which gradually became pale green with decrease of the C_{60} amount, probably due to absorption of C_{60} at near ultraviolet light region or tiny change of crystal lattice. (Fig. 27-29)

For the Fig. 27, reflection spectra of colloidal crystals formed in acetonitrile at $\phi =$ 0.147, and decrease with the decrease of amount of C_{60} tethered on poly(MMA--*co*-AEMA) grafted silica nano-particels, the reflection spectra of colloidal crystals at $\phi = 0.136$, $\phi = 0.122$ $\phi = 0.114$ $\phi = 0.106$, respectively. (Fig. 28,29). Meanwhile, distinct reflection peaks due to Bragg diffraction was observed 500nm, 518nm, 530nm, 538nm, 550nm, respectively. As follow increase with the decrease of amount of C_{60} tethered on poly(MMA--*co*-AEMA) grafted silica nano-particels, as shows in Fig. 27-29.

In Table 8, critical volume fractions of C_{60} tethered poly(MMA-*co*-AEMA) grafted

Table 8 Critical volume fraction (ϕo) of C60/ polymer-grafted SiO2, 4, in colloidal crystallization in acetonitrile

Particles	m/n	Mn	A.P. mg/g-SiO$_2$	ϕo DMF	ϕo CH$_3$CN
1	2/1	11,000	57	0.071	0.024
2	4/1	13,000	50	0.060	0.022
3	6/1	15,000	42	0.059	0.021
4	9/1	16,000	50	0.048	0.020
5	14/1	24,000	48	0.035	0.018

Table 9 Inter-particle distances in colloidal crystals of C_{60}/polymergrafted silica in CH_3CN

Particle	Volume fraction	d_{cald}/nm	$\lambda max/nm$	d_{obs}/nm
1	0.147	229	500	222
2	0.136	235	518	231
3	0.122	244	530	237
4	0.114	250	538	241
5	0.106	256	548	248

with silica nano-particles, ϕo, being minimal volume fraction in the crystallization in

CH$_3$CN and DMF were listed. Values of φo for colloidal crystallization in CH$_3$CN were in the range from 0.018 to 0.022, being mostly comparable in the crystallization of poly(MMA)-grafted silica. The values almost no change means that the crystallization almost no shape change too.

However, values of φo for colloidal crystallization in DMF in the range from 0.035 to 0.071, being twice with C$_{60}$ amounts on silica from 1.896 to 7.374 mg/g-SiO$_2$.It was suggested that the C$_{60}$ amounts on silica intensity influence of colloidal crystal in DMF. In the other words, these are a stronger interaction between C$_{60}$ with DMF than CH$_3$CN. The specific reasons for the phenomenon were still unclear.

In Table 9, inter-sphere distances, dobs and dcal, in colloidal crystals of C$_{60}$ tethered poly(MMA-*co*-AEMA) grafted with silica nano-particles in CH$_3$CN were summarized. The observed values of dobs estimated by Eq. (4) were well coincident with dcal, which were evaluated on postulation of fcc-closed packing from volume fraction of the particles by Eq. (1).[34] Therefore, these results indicated that the colloidal crystallization took place based on electrostatic repulsion between the particles to form fcc-closed packing, as well as ones of colloidal silica in aqueous solution. Colloidal crystallization of spherical particles in solution predominantly holds stable fcc structure rather than bcc packing.[34]

Conclusions

Colloidal crystallization of C$_{60}$/polymer/SiO$_2$ particles was observed in CH$_3$CN, and DMF. Critical volume fraction in the crystallization was in the range from 0.018 to 0.024 and from 0.035 to 0.071, respectively. It was suggested that these are a stronger interaction between C$_{60}$ with DMF than CH$_3$CN. It was suggest the application potential in sensor. On ther hands, color of the crystals of C$_{60}$ tethered

poly(MMA-*co*-AEMA) grafted with silica nano-particles with much amount of

tethered C_{60} was dark green, which gradually became pale green with decrease of the

C_{60} amount. For this result that suggest the application potential of C_{60} tethered

poly(MMA-*co*-AEMA) grafted with silica nano-particles in optical area.

Inter-sphere distances in the colloidal crystals mostly agreed with calculated values

on assumption of fcc-closed packing. Therefore, it was suggested that the

crystallization occurred due to electrostatic repulsion between the particles as well as

those of colloidal silica particles in aqueous solution.

References

1 Holtz JH, Asher SA. *Nature*,**1997**, 389,829–832.

2 Reese C.E., Mikhonin A.V., Kamenjicki M., Tikhonov A., Asher S.A.,*J Am Chem Soc.* **2004**, 126,1493–1496

3 Muscatello, M.M.W., Stunja, L.E., Thareja, P., Wang, L., Bohn, J. *Macromolecules*,**2009** 21,4403–4406.

4 Xia ,Y., Gates, B., Yin ,Y., Lu ,Y. *Adv Mater*, **2000**, 12, 693-713.

5 Lawrence, J.R., Ying, Y., Yiang, P., Foulger S.H., *Adv Mater*, **2006**, 18, 300–303.

6 Park J.H., Ohoi W.S., Koo H.Y., Kim D.Y. *Adv Mater,* **2005**, 17, 879-885.

7 Zhou J., Cai T., Tang S.,Marquez M., Hu Z. *Langmuir,* **2006,** 22:863–866.

8 Li Y., Kunitake T., Fujikawa S., Ozasa K. *Langmuir*,**2007**, 23,9109–9113.

9 Zhou Z., Yan Q., Li Q., Zhao X.S.   *Langmuir*, **2007**, 23, 1473–1477.

10 Hosein I.D., Lindell C.M. *Langmuir,* **2007,**23, 2892-2897.

11 Weekes S.M., Ogrin F.Y., Murray W.A., Keatley P.S.   *Langmuir,***2007***,* 23,1057–1060.

12 Camargo P.H., Lee Y.H., Jeong U., Zou Z., Xia Y. *Langmuir,***2007***,* 23:2985–2992.

13 Nakamura H., Ishii M. *Langmuir* ,**2005**, 21, 11578–11581.

14 Nakamura H., Mitsuoka T., Ishii M. *J Appl Polym Sci*,**2006**, 102, 2308–2314.

15 Kumada M., Watanabe M., Takeoka Y. *Langmuir* ,**2006**, 22,4403–4407.

16 Sakai T., Takeoka Y., Seki T., Yoshida R. *Langmuir,***2007**, 23, 8651–8654.

17 Toyotama A., Yamanaka J., Shinohara M., Onda S., Sawada T., Yonese M., Uchida F. *Langmuir*,**2009**, 25,589–593.

18 Evanoff D.D., Hayes S.E., Ying Y., Shim G.H., Lawrence J.R., Carroll JB, Roeder R.D., Houchins J.M., Huebner C.F., Foulger S.H. *Adv Mater,***2007**, 19, 3507–3512.

19 K. Yoshinaga, M.Chiyoda, T. Okubo. Colloids Surf,2002, 204,285–293

20 K. Yoshinaga, K. Fujiwara,Y. Tanaka, M. Nakanishi, M. Takesue. Chem Lett. 2003,32,1082–1083

21 K.Yoshinaga, M. Shigeta, S. Komune, E. Mouri, A. Nakai. Colloids Surf B,2007,54, 108–113

22 Yoshinaga K, Mouri E, Ogawa J, Nakai A, Ishii M, Nakamura H; Colloid Polym Sci ,2004,283,340–343

23 Yoshinaga K, Fujiwara K, Mouri E, Ishii M, Nakamura H Langmuir ,2005,21, 4471–4477

24 Yoshinaga K, Satoh S,Mouri E, Nakai A; Colloid Polym Sci ,2006,285,694–698

25 Ma Z,WatanabeM,Mouri E, Nakai A, Yoshinaga K, Colloid Polym Sci,2011, 289,85–91

26 Yoshinaga K, Chiyoda M, Yoneda A, Nishida H, Komatsu M ;Colloid Polym Sci,1999, 277,479-482

27 Dresselhaus M.S., Dresehaus G., Eklund P.C. Academic, San Diego,**2009**

28 Bonifazi D., Enger D., Diedrich F. *Chem Soc Rev*,**2007**, 36,390–444.

29 Lee J.K., Ma W.L., Brabec C.J., Yuen J., Moon J.S., Kim J.Y., Lee K., Bazan G.C., Heeger A.J. *J Am Chem Soc,***2008,** 130, 3619–3623.

30 Fernandez G., Sanchez L., Veldman D., Wienk M.M., Atienza C., Guldi D.M., Janssen R.A.J., Martin N., *J Org Chem ,***2008**, 73, 9–3196.

31 Yan H., Chen S., Lu M., Zhu X., Li X., Wu D., Tu Y., Zhu X. *Mater Horiz ,***2014,**1 , 247–250.

32 Okubo T., Okada S. *J Colloid Interface Sci,* **1998,** 204, 198-204.

33 Okubo T. *Colloid Surf A,* **1996,** 109, 77-88.

Chapter 4

Preparation of silica-tethered polymer-grafted graphene and determination of dispersion

4.1 Introduction

Graphene, a single-layer sp^2-bonded two-dimensional carbon atom with a benzene-ring structure, has many unique physical, chemical and mechanical properties, has emerged in recent years as a novel and important class of materials.[1] The quantum hall effect (QHE), high carrier mobility at room temperature ($\sim$10 000 cm^2 V^{-1} s^{-1}),[1] large theoretical specific surface area (2630 m^2 g^{-1}),[2] good optical transparency ($\sim$97.7%),[3] high Young's modulus ($\sim$1 TPa)[4] and excellent thermal conductivity (3000–5000 W m^{-1} K^{-1}).[5] In order to exploit these properties in various applications area, reliable and versatile synthetic technique has been researched to prepare graphene and its derivatives. One possible route would be incorporate graphene in a composite material. Up to now, graphene-based composites have been successfully made with inorganic nanostructures[6-13], organic crystals[14,15], polymer[16-19], metal-organic frameworks (MOFs)[20-22], biomaterials[23-24], and carbon nanotubes (CNTs)[25-26] were intensively explored in applications.

The most common approach to graphite exfoliation is oxidation to graphite oxide (GO) by strong oxidizing agents[27,28]. The partial restoration of the graphitic structure in accomplished by subsequent chemical reduction to chemically converted graphene (CCG)[29-31], however the graphitic structure is not fully restored, and significant defects are introduced. Moreover, CCG is apt to aggregation.[29,30]Although the dispersion of graphene has been reported using N,N-dimethylformamide (DMF)[32] and N-methylpyrrolidone (NMP)[33], the concentrations are low ($<$0.01 mg.mL^{-1}).

The Chrostopher E. reported a pristine graphene was prepared by exfoliating graphite in *o*-dichlorobenzene (DCB), a process that has been shown to produce graphene atoms in high yield. The choice of ODCB for graphite exfoliation was based on several criteria. First, ODCB is a common reaction solvent for fullerenes and is known to form stable SWNT dispersions presumably as a result of efficient via π-π interaction. Second, ODCB is a convenient high-boiling aromatic and is compatible with a variety of reaction chemistries. Third, Coleman and-*co*-workers have suggested that good solvents for graphite exfoliation should have surface tension values of 40-50 mJ m^{-2}. ODCB's surface tension is 36.6 mJ m^{-2}. Finally, ODCB, being aromatic, is able to interact with graphene via π-π stacking. [34]

Recently, some simple and general method for the covalent functionalization of pristine graphene was reported. The approach is based on azido groups, which upon photochemical and thermal activation, is converted to the C=C addition reaction the sp^2 C network in graphene to form the aziridine adduct. In this regard, we have successfully achieved polymer-grafted silica in organic solvents.[35-36]

In **chapter 4**, we have done a basic study of a graphene − polymer /SiO$_2$ system, polymer-grafted silica spheres-tethered graphene nano-sheet composite material, which were prepared by the reaction of graphene with 4-azidobenzoyl groups introduced in poly (methylmethacrylate-*co*-2-hydroxyethyl methacrylate), synthesized *via* a radical copolymerization, followed by esterification of 2-hydroxyethyl metharylate moieties with 4-azidobenzoyl chloride and grafted with colloidal silica. We found that the graphene/poly(MMA-*co*-AEMA)/SiO$_2$ was well dispersion in many solvents

4.2 Experimental

4.2.1 Preparation of graphene

Graphene were prepared by graphite particles (50mg) ODCB (20 ml) for 1h using a sonication probe. The mixture was settled for 1 day, and the supernatant was centrifuged at 4,400 rpm for 30min. The upper solution was collected and was used for the subsequent reactions. To determine the concentration of grapheme flakes, the solution was deposited by vacuum-filtering ODCB dispersions through alumina membranes, and dried under vacuum at 100 ^{o}C overnight.

4.2.2 Reaction of graphene with poly(MMA-*co*-AEMA)-grafted silica

Into 20 mL ODCB-graphene solution and 1.0 g composite poly(MMA-*co*-AEMA) /SiO$_2$ was put, and the mixture was stirred at 110 ^{o}C under a nitrogen atmosphere for 30 h.   Centrifugal separation of resulting particles and drying under reduced pressure gave 0. 90g composite graphene/Poly(MMA-*co*-AEMA)/SiO$_2$.

4.2.3 Determination of Structural of polymer-grafted silica spheres-tethered graphene

The morphology of graphene and polymer/SiO$_2$-grphene composite materials was observer by scanning electron microscory (SEM).The crystal structures of the samples were identified by X-ray diffraction (XRD) and Raman

4.2.4 Determination of graphene on graphene/poly(MMA-*co*-AEMA)/SiO$_2$

Amounts of grafted polymer on poly(MMA-*co*-AEMA)/SiO$_2$ were determined by weight decrease during elevation from 170°C to 420°C on a thermogravimetric analysis. Amount of graphene tethered on graphene/poly(MMA-*co*-AEMA)/SiO$_2$ was also determined by weight loss(W graphene),corresponding to grapheme ignition, during elevation from 500°C to 800°C.
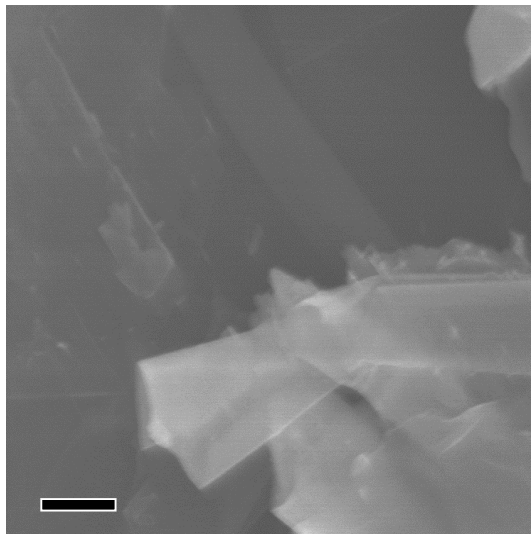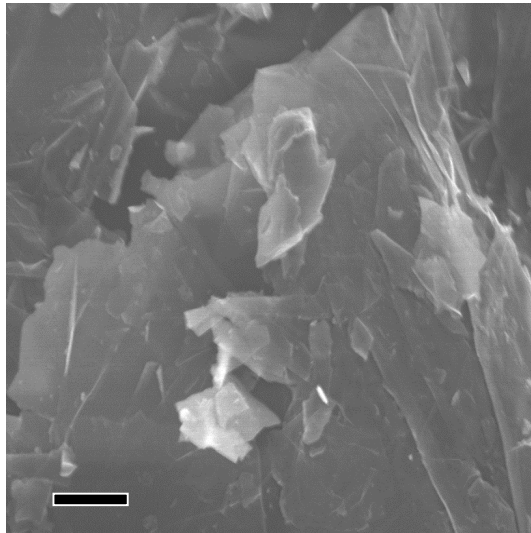
Fig. **30 SEM images of synthesized graphene**

4.2.5 XPS of graphene/poly(MMA-*co*-AEMA)/SiO₂

X-Ray photoelectron spectroscopy (XPS) studies were carried out on a Surface Science Instruments S-probe spectrometer.. The X-ray spot size used in these experiments was approximately 800 μm × 800 μm. Pressure in the analytical chamber during spectral acquisition was less than 5×10^{-9} Torr. The take-off angle (the angle between the sample normal and the axis of the analyzer lens) was 55°. Spectra used to determine surface elemental compositions were acquired at an analyzer pass energy of 150 eV. The high-resolution spectra were acquired at an analyzer pass energy of 50 eV. The XPS results are average values from analyzing three spots on at least two replicates of each sample type

4.2.6 Determination of dispersion of graphene/poly(MMA-*co*-AEMA)/SiO$_2$

The dried product was first ground with a mortar and pestle and then added to the solvent and sonicated in an ultrasound bath cleaner for 1h.To allow direct comparisons between the dispersing behavior of the different solvents, a certain amount of solvent in such a way that the resulting nominal concentration was adjusted to 0.5 mg mL^{-1} for all of the solvents. In all of the solvents, the water content was below 0.1%.

4.3 Results and discussion

Determination of graphene synthesis and SiO$_2$/polymer/graphene synthesis

As mentioned in the Experiment Section, for the SEM (Fig. 30), shows few-layer graphene and small flakes stacked on top. However, due to the aggregation effect under the dry condition, there is difficult to evaluate the layer number of

NONE   SEI   5.0kV   X10,000   WD 7.6mm   1 μm
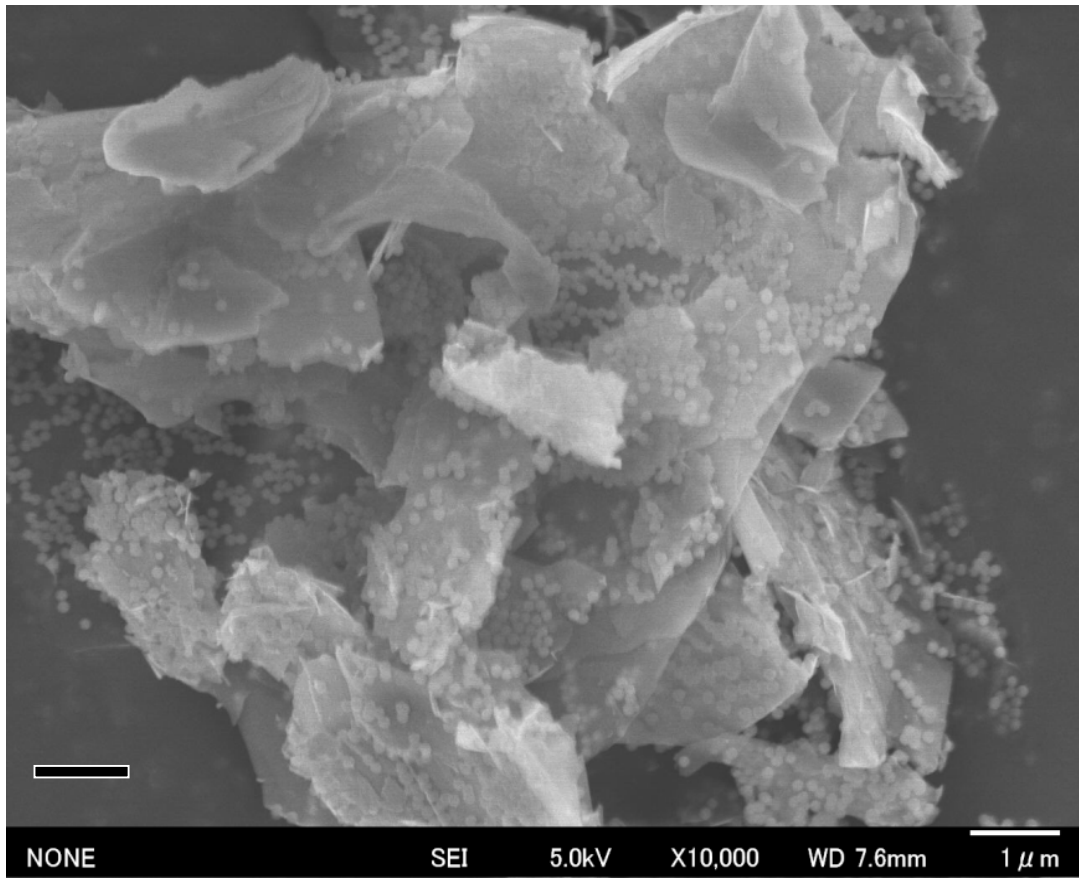
Fig. **31 SEM images of SiO$_2$ tethered**

poly(MMA-*co*-AEMA) grafted graphene

32a

32b
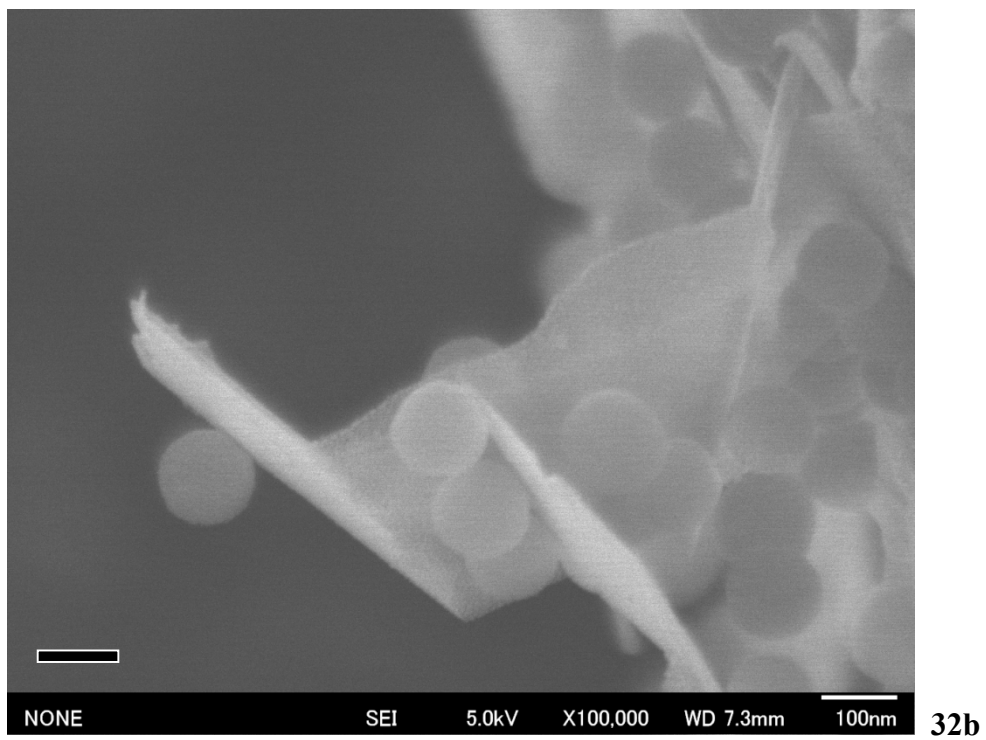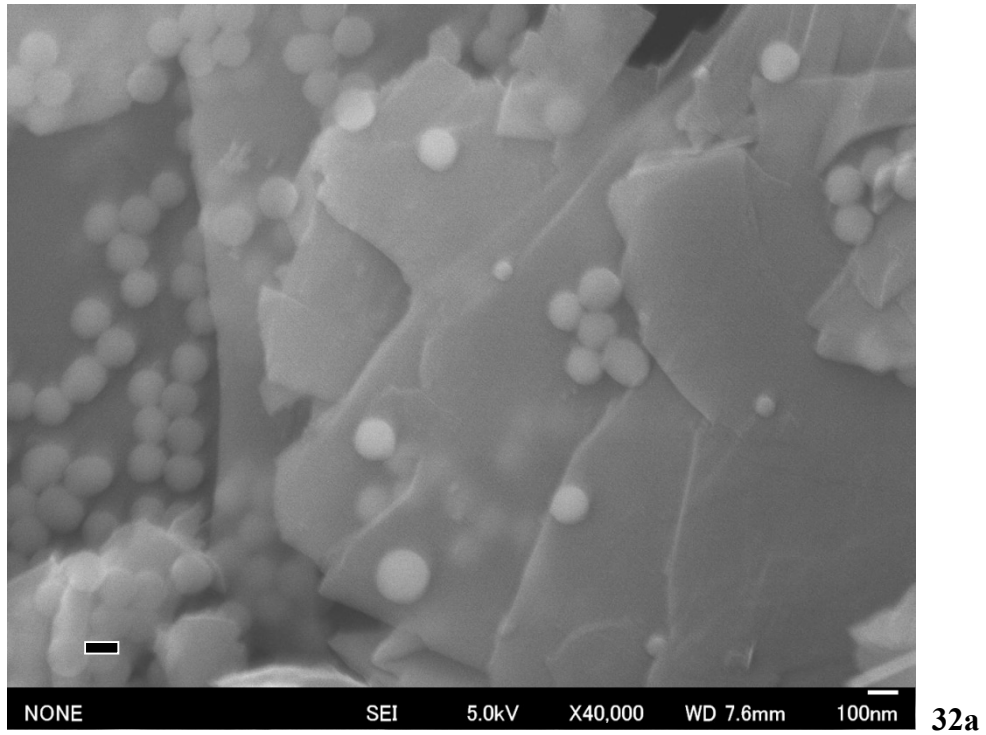
Fig. **32 High enlargement factor SEM images: ×40,000 (32a) ×100,000(32b)**
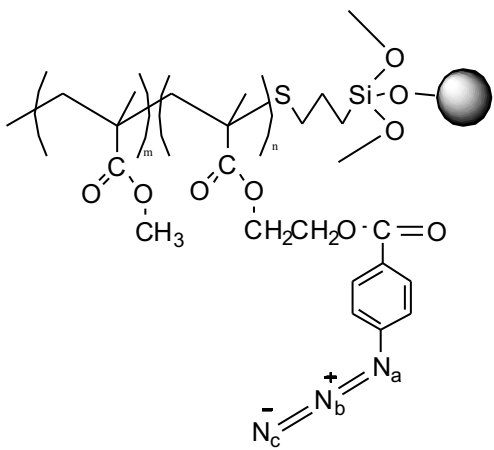
graphene exactly.

The reaction of graphene with poly(MMA-*co*-AEMA)/SiO$_2$ was carried out in ODCB at 90 ^{o}C under a nitrogen atmosphere for 30h. After that time, the resulting particles were homogenized for 1 hour followed by cup-horn sonication for 30minutes and centrifugal washed with ODCB 30 minutes at 4400rpm. The upper solution has a few back suspended matters, we surmise that it was non-reaction graphene. As for the possible presence of free-SiO$_2$, remove the ODCB and drying under reduced pressure, add deionized-water and H-form type strongly acid cation exchange resin, settled for 24h. The free-SiO$_2$ conversion to hydrophilic SiO$_2$, which can be filtered by 0.45um hydrophilic membrane. When there is no white precipitate appeared in the filtrate, pure polymer grafted SiO$_2$-tethered graphene nano-sheet were observed. For the SEM (Fig. 31), it was exhibited that the SiO$_2$ grafted on the silica surface.

Before the he reaction between the Poly(MMA-*co*-AEMA) grafted with silica and the graphene ,we have probably estimate that the graphene is few layers. However, we could not estimate the layer number. For the SEM picture Fig. 32a, we could clear see that the silica nano-particles at reverse side, it was suggested that the graphene very thin. From the SEM picture Fig. 32b, it was suggest that the thich of graphene could be just 2nm.

The evidence on the covalent bond formation between graphene and silica-tethered polymer-grafted graphene was provided by X-ray photoelectron spectroscopy (XPS).The fluorine to nitrogen atomic ratios were calculated from XPS determined surface elemental compositions before and after the reaction between the Poly(MMA-*co*-AEMA) grafted with silica and the graphene. Table 8 summarized the XPS peak assignment of the N1s core level spectrum of the Poly(MMA-*co*-AEMA) grafted with silica. Although the concentration on the low side, three peaks were

Table 10. XPS Peak Assignments of the N 1s Core Level Spectrum of the Polymer/SiO₂

	Binding Energy, eV		
	N_a	N_b	N_c
	401.5	404.1	398.7
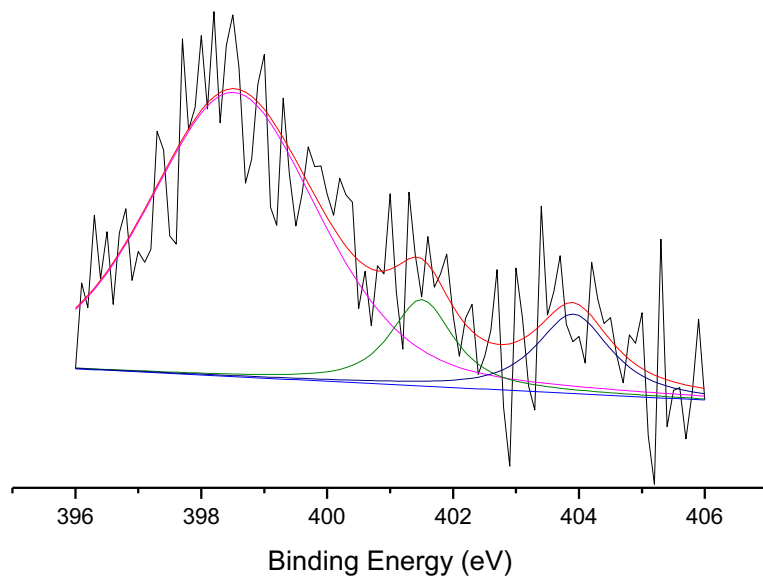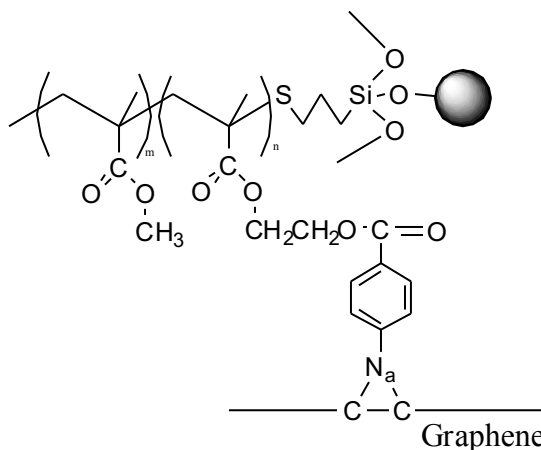
Binding Energy (eV)

Fig. **33. The corresponding XPS N1s core level spectra of the Polymer/SiO₂**

Table 11. XPS Peak Assignments of the N 1s Core Level Spectrum of the Graphene/Polymer/SiO₂

	Binding Energy, eV		
	N_a	N_b	N_c
	400.5	None	None
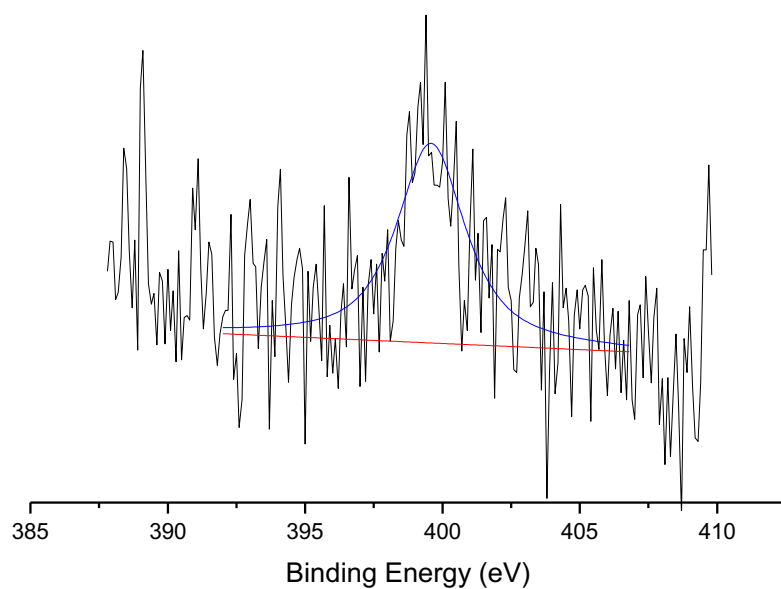
Fig. **34. The corresponding XPS N1s core level spectra of the Graphene Polymer/SiO₂**

Fig. **35 Pictures of graphene/poly(MMA-*co*-AEMA)/SiO$_2$**

dispersion in water with different concentration.

exhibited in the spectrum of the Poly(MMA-*co*-AEMA) grafted with silica(Fig. 34). The two BE peaks at 404.1eV and 398.7eV, which are originated from N_b and N_c of the N_3 group ($^-N_a=N_b{}^+=N_C{}^-$).Another BE peak at 401.5eV, which are originated from N_a of the N_3 group ($^-N_a=N_b{}^+=N_C{}^-$). It was suggested that Poly(MMA-*co*-AEMA) grafted with silica was synthesized succeed.

Table 11 summarized the XPS peak assignment of the N1s core level spectrum of the polymer grafted SiO_2-tethered graphene. Although the concentration on the low side, just one peaks were exhibited in the polymer grafted SiO_2-tethered graphene (Fig. 35).The peak at 400.5eV, it is attributed to the N atom from N of the

(C-N-C), which is due to the decomposition of the azide. Before the reaction, the two BE peaks at 404.1eV and 398.7eV, which are originated from N_b and N_c of the N_3 group ($^-N_a=N_b{}^+=N_C{}^-$), both peaks decreased significantly in intensity after reaction with the graphene flakes.The change of the N 1s spectrum after reaction with the graphene overlayer is consistent with conversion of Ar-N_3 to Ar-N (i.e., loss of central and outer N atoms).

Determination of dispersion of polymer grafted SiO$_2$-tethered graphene

As is known to all, graphene is difficult to disperse in many solvents, especially in water or ethanol. We found that the graphene/poly(MMA-*co*-AEMA)/SiO$_2$ was well dispersion in water. As show as Fig. 35 the graphene/poly(MMA-*co*-AEMA)/SiO$_2$ were well dispersion, from 0.128mg/ml to 1.024mg/ml. It was expected to prepare low cost and stable performance conductive materials.

As mentioned in the Experimental Section, the as-prepared graphene/poly(MMA--*co*-AEMA)/SiO$_2$ was dispersed in water and 8 organic solvents to a nominal concentration of 0.5mgmL^{-1} with the aid of bath ultrasonication, and the

	DMF	Methanol	Ethanol	Ethylene glycol
Just sonicated				
After 24h				
After 48h				

Fig. **36 Time course of graphene/poly(MMA- -*co*-AEMA)/SiO₂ in DMF, Methanol, Ethanol and Ethylene glycol.**

	Acetone	**THF**
Just sonicated		
After 24h		
After 48h		

Fig. **37 Time course of graphene/poly(MMA- -*co*-AEMA)/SiO₂ in Acetone and THF**

	Pyridine	**Cyclo-hexane**
Just sonicated		
After 1h		
After 6h		

Fig. **38 Time course of graphene/poly(MMA- -*co*-AEMA)/SiO₂ in Pyridine and Cyclohexane.**

dispersions were then allowed to settle for several days. Fig. 36-38 shows digital

pictures of all of the dispersions immediately after sonication (top) and 48h after

sonication (bottom). For the just sonicated samples, it can be noticed that

graphene/poly(MMA--co-AEMA)/SiO_2 could be dispersed in almost all of the solvents,

except cyclohexane (Fig. 38). However, acetone, THF and pydine dispersions

displayed only short-term stability and precipitated completely in a matter of hours to a

few days(Fig. 37), especially completed in 1h. By contrast, as prepared

graphene/poly(MMA -co-AEMA)/SiO_2 dispersions in four organic solvents (ethylene

glycol, DMF, methanol, ethanol) (Fig. 36) were seen to exhibit long-term stability

comparable to that observed for the dispersion of the same material in water.

In the case of water and the four mentioned organic solvents, a small amount of

precipitate was seen to develop only within the first few days after sonication

(no additional precipitation was observed after such time), which we attribute to

polymer grafted SiO_2-tethered graphene material that could not be sufficiently

exfoliated during the 1 h sonication period. In fact, longer sonication times tended to

decrease the amount of precipitate. Under identical preparation conditions, it was

observed that ethylene glycol and THF dispersions yielded somewhat larger amounts of

precipitate in relation to those of water, DMF dispersions, suggesting that the former

solvents possess a comparatively smaller dispersing ability.

The colloidal nature of the resulting polymer grafted SiO_2-tethered graphene

dispersions is further confirmed by two experiment typically conducted in colloid

science: investigations of the Tyndall effect and the salt effect.(Fig. 39,40) A dilited

polymer grafted SiO_2-tethered graphene dispersion gives rise to the Tyndall effect, in

which a laser beam passing through a colloidal solution leaves a discernible track as a

result light scattering. Adding an electrolyte solution such as sodium chloride into a
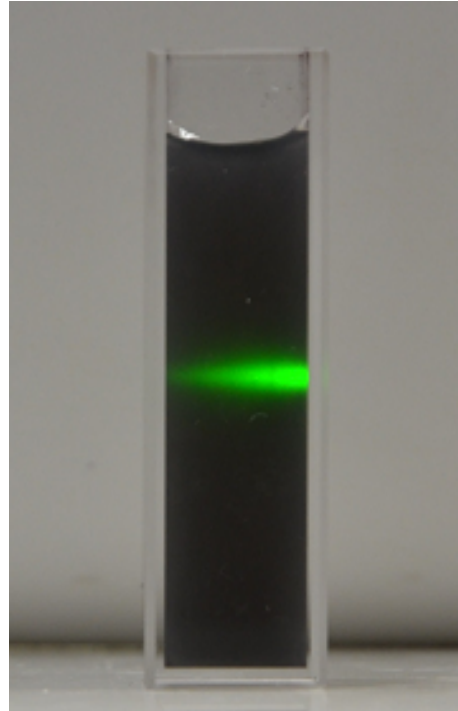
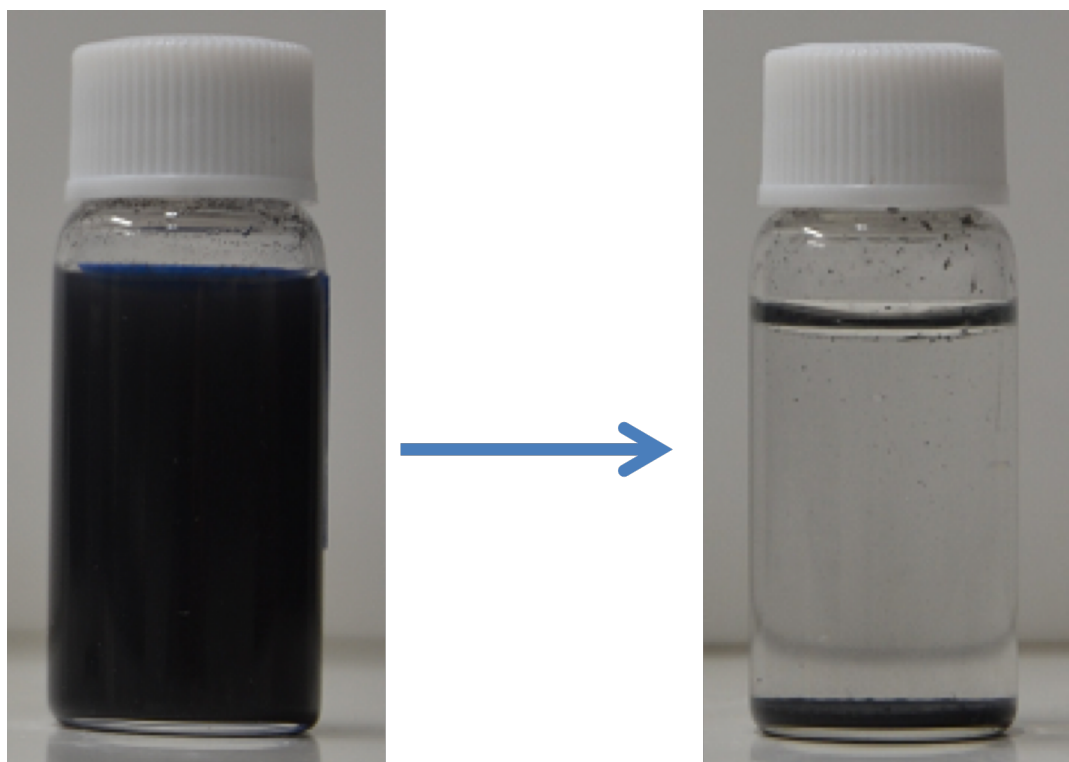Fig. **39 The Tyndall effect of graphene/poly(MMA- -*co*-AEMA)/SiO₂ in water.**

NaCl

Instant

Fig. **40 The salt effect of graphene/poly(MMA- -*co*-AEMA)/SiO₂.**

polymer grafted SiO$_2$-tethered graphene dispersion leads to immediate coagulation.

Conclusion

We have done a basic study of a graphene – polymer /SiO$_2$ system, polymer-grafted silica spheres-tethered graphene nano-sheet composite material, which were prepared by the reaction of graphene with 4-azidobenzoyl groups introduced in poly (methylmethacrylate-*co*-2-hydroxyethyl methacrylate).For the XPS and SEM, it was suggested that few layer silica-tethered polymer-grafted graphene were obtained, and no aggregation occurred. We also found that the polymer grafted SiO$_2$-tethered graphene was well dispersion in water and some organic solvents. By contrast, graphene just could disperse in little solvent. It was suggested that the dispersion was completely changed with tethered lots of silica.

References

1   Novoselov K. S., Geim A. K., Morozov S. V., Jiang D., Zhang Y., Dubonos S. V., Grigorieva I. V.   and Firsov A. A., *Science*, **2004**, 306, 666–669

2   Stoller M. D., Park S., Zhu Y., An J. and Ruoff R. S., *Nano Lett,* **2008,** 8, 3498–3502

3   Nair R. R., Blake P., Grigorenko A. N., Novoselov K. S., Booth T. J., Stauber T., Peres N. M. R. and Geim A. K., *Science*, **2008**, 320, 1308–1308.

4   Lee C., Wei X. D., Kysar J. W. and Hone J., *Science*, **2008**, 321, 385–388.

5   Balandin A. A., Ghosh S., Bao W., Calizo I., Teweldebrhan D., Miao F. and Lau C. N., *Nano Lett*., **2008**, 8, 902–907

6   Wu S., Yin Z., He Q., Huang X., Zhou X. and Zhang H., *Phys. J.Chem. C*, **2010**, 114, 11816–11821.

7   Yin Z., Wu S., Zhou X., Huang X., Zhang Q., Boey F. and Zhang H. *Small*, **2010**, 6, 307–312.

8   Zhou X., Huang X., Qi X., Wu S., Xue C., Boey F. Y. C., Yan Q., Chen H. and Zhang H. *J. Phys. Chem. C*, **2009**, 113,10842–10846.

9   Sudibya H. G., He Q., Zhang H. and Chen P., *ACS Nano*, **2011**, 5, 1990–1994.

10 Muszynski R., Seger B. and Kamat P. V., *J. Phys. Chem. C*, **2008**,112, 5263–5266.

11 Shi W., Zhu J., Sim D. H., Tay Y. Y., Lu Z. Y., Zhang X. J., Zhang H., Hng H. H. and Yan Q. *J. Mater. Chem*., **2011**, 21, 3422–3427.

12 Zhu J., Zhu T., Zhou X., Zhang Y., Lou X. W., Chen X., Chen H., Zhang H., Hng H. H., Ma J. and Yan Q., *Nanoscale*,**2011**, 3, 1084–1089.

13 Huang X., Li S., Huang Y., Wu S., Zhou X., Li S., Gan C. L., Boey F., Mirkin C. A.   and Zhang H., *Nat. Commun*., **2011**, 2, 292

14   S. Wang, B. M. Goh, K. K. Manga, Q. Bao, P. Yang andK. P. Loh, *ACS Nano*, **2010**, 4, 6180–6186.

15 T. H. Han, W. J. Lee, D. H. Lee, J. E. Kim, E. Y. Choi and S. O. Kim, *Adv. Mater.*, **2010**, 22, 2060–2064.

16 X. Qi, K.-Y. Pu, H. Li, X. Zhou, S. Wu, Q.-L. Fan, B. Liu,F. Boey, W. Huang and H. Zhang, *Angew. Chem., Int. Ed*., **2010**,49, 9426–9429

17 X. Qi, K. Y. Pu, X. Zhou, H. Li, B. Liu, F. Boey, W. Huang and H. Zhang, *Small*, **2010**, 6, 663–669.

18 H. F. Yang, Q. X. Zhang, C. S. Shan, F. H. Li, D. X. Han andL. Niu, *Langmuir,* **2010**, 26, 6708–6712.

19 T. Ramanathan, A. A. Abdala, S. Stankovich, D. A. Dikin,M. Herrera-Alonso, R. D. Piner, D. H. Adamson,H. C. *Nat.Nanotechnol*., **2008**, 3, 327–331.

20 M. Jahan, Q. Bao, J.-X. Yang and K. P. Loh, *J. Am. Chem. Soc*.,**2010**, 132, 14487–14495.

21 C. Petit and T. J. Bandosz, *Adv. Funct. Mater.*, **2010**, 20, 111–118.

22 C. Petit, J. Burress and T. J. Bandosz, *Carbon*, **2011**, 49, 563–572.

23 C. H. Lu, H. H. Yang, C. L. Zhu, X. Chen and G. N. Chen, *Angew. Chem., Int. Ed.*, **2009**, 121, 4879–4881.

24 H. Chang, L. Tang, Y. Wang, J. Jiang and J. Li, *Anal. Chem.*,**2010**, 82, 2341–2346.

25 Y. Wang, Z. Li, D. Hu, C.-T. Lin, J. Li and Y. Lin, *J. Am. Chem.Soc.*, **2010**, 132, 9274–9276.

26 X. Dong, B. Li, A. Wei, X. Cao, M. B. Chan-Park, H. Zhang,L.-J. Li, W. Huang and P. Chen, *Carbon*, **2011**, 49, 2944–2949

27 Stankovich, S.et al. *Carbon,* **2007***,* 45, 1558-1565.

28 Stankovich, S et al. *J Mater. Chem.* **2006**, 16, 155-158

29 Schniepp, H. C.; Li, J.-L.; McAllister, M. J.; Sai, H.; Herrera-Alonso,M.; Adamson, D. H.; Prud'homme, R. K.; Car, R.; Saville, D. A.;Aksay, I. A. *J. Phys. Chem. B* **2006**, *110*, 8535.

30 (a) Si, Y.; Samulski, E. T. *Nano Lett.* **2008**, *8*, 1679. (b) Lomeda,. R.; Doyle, C. D.; Kosynkin, D. V.; Hwang, W.-F.; Tour, J. M. *J. Am.Chem. Soc.* **2008**, *130*, 16201. (c) Chattopadhyay, J.; Mukherjee, A.;Hamilton, C. E.; Kang, J.-H.; Chakraborty, S.; Guo, W.; Kelly, K. F.;Barron, A. R.; Billups, W. E. *J. Am. Chem. Soc.* **2008**, *130*, 5414.

31 (a) Stankovich, S.; Dikin, D. A.; Piner, R. D.; Kohlhaas, K. A.;Kleinhammes, A.; Jia, Y.; Wu, Y.; Nguyen, S. B. T.; Ruoff, R. S.*Carbon* **2007**, *45*, 1558. (b) Xu, Y.; Bai, H.; Lu, G.; Li, C.; Shi, G.*J. Am. Chem. Soc.* **2008**, *130*, 5856. (c) Li, D.; Mueller, M. B.; Gilje,S.; Kaner, R. B.; Wallace, G. G. *Nat. Nanotechnol.* **2008**, *3*, 101.

32 Blake, P.; Brimicombe, P. D.; Nair, R. R.; Booth, T. J.; Jiang, D.;*Nano Lett.* **2008**, *8*, 1704.

33 Hernandez, Y.; Nicolosi, V.; Lotya, M.; Blighe, F. M.; Sun, Z.; De,S.; McGovern, I. T.; Holland, B.; Byrne, M.; Gun'Ko, Y. K.; *Nanotechnol.* **2008**, *3*, 563.

34 Christipher E., Hamiton J.R.L., Zhengzong S., James M.T. and Andrew R.B. *Nano Lett,* **2009**, 9, 3460-3462.

35 LiHong L., Gilad Z., David G.C., Raj S., Michael M.L. and Mingdi Y. *J Mater Chem*, **2010,** 20, 5041-5046.

36 LiHong L., Michael M.L. and Mingdi Y. *Nano Lett,***2010**, 10, 3754-3756

General Conclusions

This thesis has presented a novel approach to connect the π-conjugated carbon molecules to nano-particles *via* difunctional polymer, which owning two function on side chain and the terminal, respectively. Targeting conveniently adjust the ratio of carbon molecules to nano-particles and fine-turning the proprieties, to develop this area further.

Fullerene(C_{60})-tethered polymer-grafted silica spheres were successfully synthesized via reaction of C_{60} with 4- azidobenzoyl group in poly(MMA-*co*-HEMA) grafted on silica. Bindings of C_{60} on poly(MMA-*co*-HEMA)-grafted silica were confirmed by appearance of characteristic resonance peaks at 120–142 *ppm*, assignable to carbon atoms of C_{60}, on a ^{13}C CP/MAS NMR spectrum. The reaction afforded bindings of C_{60} in the range from 2.63 to 10.2 μmol/g-SiO_2, corresponding to $0.44×104$ to $1.71×104$ molecules/particle,on the polymer-grafted silica. Colloidal crystallization of C_{60}/polymer/SiO_2 particles was observed in CH_3CN, and critical volume fraction in the crystallization was in the range from 0.018 to 0.024. Inter-sphere distances in the colloidal crystals mostly agreed with calculated values on assumption of fcc-closed packing. Therefore, it was suggested that the crystallization occurred due to electrostatic repulsion between the particles as well as those of colloidal silica particles in aqueous solution.

We have done a basic study of a graphene – polymer /SiO_2 system, polymer-grafted silica spheres-tethered graphene nano-sheet composite material, which were prepared by the reaction of graphene with 4-azidobenzoyl groups introduced in poly (methylmethacrylate-*co*-2-hydroxyethyl methacrylate).For the XPS and SEM, it was suggested that few layer silica-tethered polymer-grafted graphene were obtained, and

no aggregation occurred. We also found that the polymer grafted SiO_2-tethered graphene was well dispersion in water and some organic solvents. By contrast, graphene just could disperse in little solvent. It was suggested that the dispersion was completely changed with tethered lots of silica.

Publication List

1. Photocatalytic reduction of CO_2 over exposed-crystal-face-controlled TiO_2 nanorod having a brookite phase with-*co*-catalyst loading.
   Applied Catalysis B: Environmental, vol.152-153, pp.309-316
   Teruhisa Ohno, Takayoshi Higo ,Naoya Murakami, Hirofumi Saito,
   Qitao Zhang, **Yin Yang** ,Toshiki Tsubota

2. Photocatalytic reduction of CO_2 over a hybrid photocatalyst Composed of WO_3 and graphitic carbon nitride (g-C_3N_4) under visible light.
   Journal of CO_2 Utilization, Vol.6, pp.17-25
   Teruhisa Ohno, Naoya Murakami, Takahiro Koyanagi, **Yin Yang**

3. Inclusion of fullerene in polymer chains grafted on silica Nanoparticles in an organic solvent
   Polymer joumal, Vol.46, pp.623-627
   Kohji Yoshinaga, **Yin Yang**, Teruhisa Ohno, Suguru Motokucho Ken Kojio

4. Porous Cerium Dioxide Hollow Spheres and their Photocatalytic Performance.
   RSC Adv., Vol.4, pp.62255-62261   AS
   Yuan Saisai, Zhang Qitao, Xu Bin, Jin Zhengyuan, Zhang ya, **Yang Yin**, Zhang Ming, Ohno Teruhisa

5. Dependence of photocatalytic activity on aspect ratio of a brookite TiO_2 nanorod and drastic improvement in visible light responsibility of a brookite TiO_2 nanorod by site-selective modification of Fe^{3+} on exposed faces.
   Journal of Molecular Catalysis A: Chemical, Vol.396, pp.261–267
   Teruhisa Ohno; Hirofumi Saito; Takayoshi Higo; Naoya Murakami; Zhengyuan Jin; **Yin Yang**; Toshiki Tsubota

6. Fabrication of morphology controlled TiO_2 photocatalyst nanoparticles and their

improvement of photocatalytic activities by Fe compounds modification.
Rare Metals, Vol. 34, pp. 291-300
Yin Yang and Teruhisa Ohno

7. Colloidal Crystallization of C_{60}/Polymer-Grafted Silica Particles in Organic Solvent
Colloid and Polymer Science, Vol. 293, pp. 2075-2081
Yin Yang, Teruhisa Ohno, and Kohji Yoshinaga